

The role of electrostriction on the stability of dielectric elastomer actuators

Massimiliano Gei*, Stefania Colonnelli*, Roberta Springhetti*

October 26, 2021

Abstract

In the field of soft dielectric elastomers, the notion ‘electrostriction’ indicates the dependency of the permittivity on strain. The present paper is aimed at investigating the effects of electrostriction onto the stability behaviour of homogeneous electrically activated dielectric elastomer actuators. In particular, three objectives are pursued and achieved: i) the description of the phenomenon within the general nonlinear theory of electroelasticity; ii) the application of the recently proposed theory of bifurcation for electroelastic bodies in order to determine its role on the onset of electromechanical and diffuse-mode instabilities in prestressed or pre-stretched dielectric layers; iii) the analysis of band-localization instability in homogeneous dielectric elastomers. Results for a typical soft acrylic elastomer show that electrostriction is responsible for an enhancement towards diffuse-mode instability, while it represents a crucial property - necessarily to be taken into account - in order to provide a solution to the problem of electromechanical band-localization, that can be interpreted as a possible reason of electric breakdown. A comparison between the buckling stresses of a mechanical compressed slab and the electrically activated counterpart concludes the paper.

Keywords: Electroelasticity, Electroactive polymers, Smart materials, Electromechanical instability, buckling actuator

1 Introduction

Dielectric elastomer (DE) devices are electrically activated smart systems that possess mechanical properties similar to those of natural muscles and therefore represent one of the most promising members within the class of the artificial muscles (Bar-Cohen, 2001; Brochu and Pei, 2010). Applications of these systems are common in the fields

*Department of Civil, Environmental and Mechanical Engineering (DICAM), University of Trento, Via Mesiano 77, I-38123 Trento, Italy; email: massimiliano.gei@unitn.it; web-page: www.ing.unitn.it/~mgei.

of mechatronics, aerospace, biomedical and energy engineering as actuators, sensors, and energy harvesters (Carpi et al., 2008a). Their operating principle is based on the deformation of a dielectric soft membrane induced by the electrostatic attraction forces arising between the charges placed on its opposite sides (Pelrine et al., 1998, 2000); such effect is proportional to the permittivity of the material, which unfortunately turns out to be very low for the typical materials in use (e.g., silicones, acrylic elastomers) with relative dielectric constants ϵ_r amounting to a few units.

While, on the one hand, research efforts are devoted to the design and realization of composite materials with significantly higher permittivities to improve the electromechanical coupling (Zhang et al., 2002; Huang et al., 2004; deBotton et al., 2007; Carpi et al., 2008b, Molberg et al., 2010; Bertoldi and Gei, 2011; Risse et al., 2012; Ponte Castaneda and Siboni, 2012; Tian et al., 2012; Gei et al., 2013), on the other hand, the nonlinear theory of homogeneous soft dielectrics is still under way, in particular, special attention deserve the issues associated with the different types of instability developing under operating conditions and those related to the intrinsic behaviour of the material, such as electrostriction and polarization saturation (Li et al., 2011a; Ask et al., 2012, 2013).

The aim of this paper is to give a contribution to the aspects just mentioned, by pursuing three main goals:

- to provide a framework accounting for electrostriction of soft DEs within the general nonlinear theory of electroelasticity. As usual in the field of soft dielectrics, electrostriction is conceived as the dependency of the relative permittivity of the material on strain: this effect, experimentally observed (Wissler and Mazza, 2007; Li et al., 2011b), must be taken into account for modelling purposes in view of the large deformations usually achieved. This phenomenon has been theoretically addressed by Zhao and Suo (2008) who employed a simple model for its characterization;
- to apply the general theory of bifurcation for electroelastic body proposed by Bertoldi and Gei (2011) to investigate (*i*) electromechanical instability in unconstrained specimens and (*ii*) diffuse-mode instabilities, including buckling-like and surface-like modes, in prestretched dielectric layers. In the aforementioned paper the focus was on layered composites (see also Nobili and Lanzoni, 2010, and Rudykh and deBotton, 2011), while the current analyses are performed on homogeneous materials, for which the two types of bifurcation are obtained on the basis of a common general criterion. Electromechanical instability on its own was extensively studied by methods developed by Zhao et al. (2007) and De Tommasi et al. (2010), while De Tommasi et al. (2013) showed that an imperfection could trigger this instability at a voltage much lower than that for a homogeneous specimen. Regarding the importance of diffuse modes, we mention that an Euler-like instability is the activation mechanism of several types of buckling-like actuators (Carpi et al., 2008a; Vertechy et al., 2012);

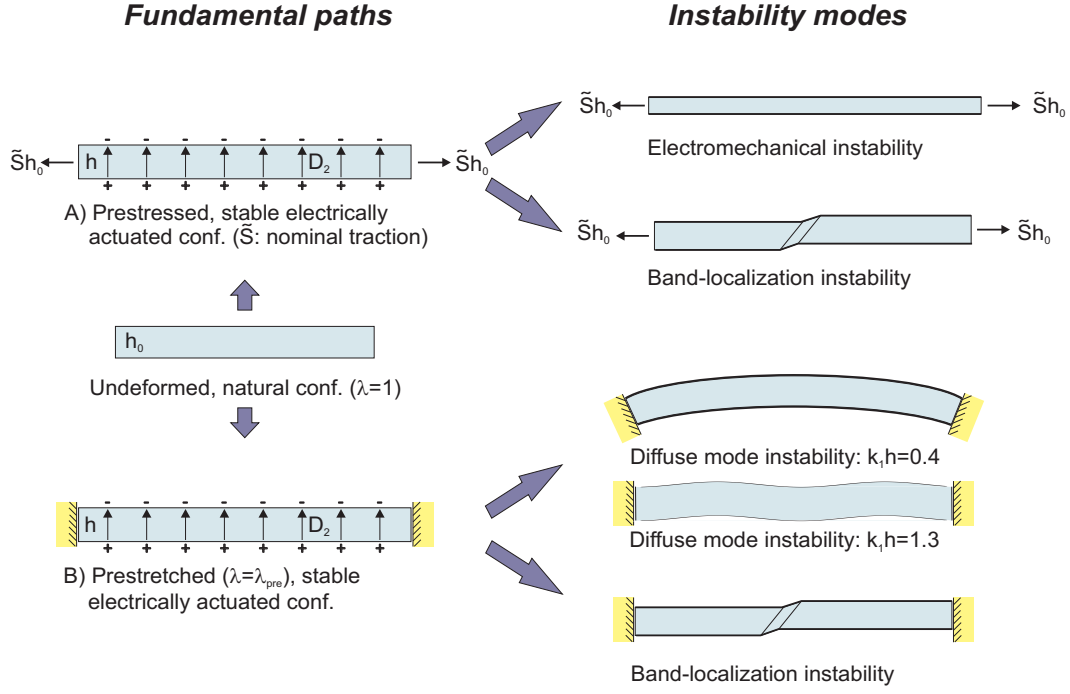


Figure 1: Sketch of the instabilities investigated in the paper for a soft dielectric layer subjected to two different electromechanical loading paths. A: the layer is electrically actuated with a constant longitudinal force $-\tilde{S}$ is the nominal traction-; B: the layer is first prestretched at a longitudinal stretch equal to λ_{pre} and then electrically actuated (h_0 and h denote the initial and the reference thickness, respectively; D_2 represents the current electric displacement field).

- to analyze band-localization instability in homogeneous DEs, in particular facing its relation with the constitutive properties of the solid. The theory developed here extends to the electroelastic domain the well-known theory of localization of deformation in nonlinear elasticity, where the existence of a localized solution of the incremental problem – concentrated within a narrow band – is sought along the loading path (Rice, 1973; Hill and Hutchinson, 1975; Bigoni and Dal Corso, 2008).

General assumptions adopted throughout the paper involve plane-strain deformation and material incompressibility. Fig. 1 reports a sketch of the investigated instabilities relevant to the homogeneous loading paths assumed for the layer that is always actuated by a given transverse electric displacement field: in the first (Path A), the prestressed specimen can freely expand under the electrical actuation, while in the second (Path B), the layer is first mechanically prestretched and successively actuated. The obtained results, well suited to a wide class of diffused acrylic elastomers, show that electrostriction plays a fundamental role in the stability behaviour of the actuators.

The paper is organized into eight sections. Sects. 2 and 3 deal with the formulation of the finite and the linearized electroelastic models, respectively. Sect. 4 introduces the considered electromechanical loading paths, while in Sect. 5 the formulation of the general theory of electroelastic bifurcations introduced by Bertoldi and Gei (2011) is

recalled and specialized to the plane-strain problem under study. The band-localization instability is discussed in Sect. 6, while all results and their interpretation are presented in Sect. 7. Finally, the conclusions are summarised in Sect. 8, while in Appendix A the components of the incremental moduli associated with the general free energy introduced in Sect. 2 are detailed.

2 Large deformations and stress state for a soft dielectric body

Here the theory of large-strain electroelasticity for a homogeneous isotropic hyperelastic body is briefly recalled, on the basis of the notion of total stress. The reader is referred to McMeeking and Landis (2005), Dorfmann and Ogden (2005), Suo et al. (2008) and Bertoldi and Gei (2011) for further details.

A system in equilibrium under external electromechanical actions is considered, including an electroelastic body occupying a region $B \in \mathbb{R}^3$, whose points are denoted by \mathbf{x} and the surrounding space $B^{\text{sur}} = \mathbb{R}^3 \setminus B$. Here the general case of the surrounding domain occupied by a different dielectric medium is briefly illustrated, while in our reference problem we assume B^{sur} corresponding to vacuum, in such case it will be denoted by B^* . The stress-free configuration of the body B^0 , whose points are labelled \mathbf{x}^0 , can be identified, such that $\mathbf{x} = \boldsymbol{\chi}(\mathbf{x}^0)$, where $\boldsymbol{\chi}$ represents a given deformation and $\mathbf{F} = \partial\boldsymbol{\chi}/\partial\mathbf{x}^0$ denotes its gradient. In the general case, the material configuration of the surrounding domain is analogously denoted by $B^{0\text{sur}}$, while no reference configuration is introduced in the case of vacuum, as the deformation gradient is not defined there.

2.1 Field equations and boundary conditions

Under the hypotheses previously introduced and assuming the absence of body forces and volume free charges, the governing equations of the system in the spatial description are:

$$\operatorname{div} \boldsymbol{\tau} = \mathbf{0}, \quad \boldsymbol{\tau}^T = \boldsymbol{\tau}, \quad \operatorname{div} \mathbf{D} = 0, \quad \operatorname{curl} \mathbf{E} = \mathbf{0} \quad (\text{in } B \cup B^{\text{sur}}). \quad (1)$$

Here $\boldsymbol{\tau}$ denotes the ‘total’ stress, while \mathbf{D} and \mathbf{E} represent the electric displacement and the electric field respectively; operators written with initial lower-case (upper-case) refer to variables defined in the present (reference) configuration. Condition (1)₄ states that \mathbf{E} is a conservative field, therefore it can be derived from a potential function $\phi(\mathbf{x})$, i.e. $\mathbf{E} = -\operatorname{grad}\phi(\mathbf{x})$, both in B and B^{sur} .

According to the considered set of boundary conditions, the charges are specified along the whole boundary ∂B , while displacements and tractions prescriptions are enforced on disjoint parts of ∂B , denoted as ∂B_v and ∂B_t , respectively, such that $\partial B_v \cup \partial B_t = \partial B$ with $\partial B_v \cap \partial B_t = \emptyset$, namely

$$[[\mathbf{v}]] = \mathbf{0}, \quad [[\boldsymbol{\tau}]]\mathbf{n} = \mathbf{t} \quad (\text{on } \partial B_t), \quad \mathbf{v} = \tilde{\mathbf{v}} \quad (\text{on } \partial B_v), \quad (2)$$

$$[[\mathbf{D}]] \cdot \mathbf{n} = -\omega, \quad \mathbf{n} \times [[\mathbf{E}]] = \mathbf{0} \quad (\text{on } \partial B),$$

where the jump operator defined on ∂B corresponds to $[[f]] = f_B - f_{B^{\text{sur}}}$, $\mathbf{v}(\mathbf{x})$ denotes the finite displacement function with prescribed values $\tilde{\mathbf{v}}$ on the restrained portion of the boundary ∂B_v , \mathbf{t} and ω represent the assigned values of the tractions on the free boundary ∂B_t and the surface charge density, respectively, while \mathbf{n} is the current outward normal to ∂B .

The Lagrangian formulation of the above setting is also required, which is based on a back-mapping of the governing equations (1) to the reference configuration $B^0 \cup B^{0\text{sur}}$. The variables involved are the first Piola-Kirchhoff total stress

$$\mathbf{S} = J\boldsymbol{\tau}\mathbf{F}^{-T} \quad (3)$$

and the material (or Lagrangian) version of the electric variables, i.e.

$$\mathbf{D}^0 = J\mathbf{F}^{-1}\mathbf{D} \quad \text{and} \quad \mathbf{E}^0 = \mathbf{F}^T\mathbf{E}. \quad (4)$$

In particular, under the same hypotheses, the field equations read now

$$\text{Div } \mathbf{S} = \mathbf{0}, \quad \mathbf{S}\mathbf{F}^T = \mathbf{F}\mathbf{S}^T, \quad \text{Div } \mathbf{D}^0 = 0, \quad \text{Curl } \mathbf{E}^0 = \mathbf{0} \quad (\text{in } B^0 \cup B^{0\text{sur}}), \quad (5)$$

thus also the electric field \mathbf{E}^0 proves to be conservative. The prescribed boundary conditions are analogous to those in (2) for the corresponding Lagrangian variables

$$[[\mathbf{v}^0]] = \mathbf{0}, \quad [[\mathbf{S}]]\mathbf{n}^0 = \mathbf{t}^0 \quad (\text{on } \partial B_t^0), \quad \mathbf{v}^0 = \tilde{\mathbf{v}}^0 \quad (\text{on } \partial B_v^0), \quad (6)$$

$$[[\mathbf{D}^0]] \cdot \mathbf{n}^0 = -\omega^0, \quad \mathbf{n}^0 \times [[\mathbf{E}^0]] = \mathbf{0} \quad (\text{on } \partial B^0),$$

where $\mathbf{v}^0(\mathbf{x}^0)$ is the Lagrangian description of the finite displacement field, \mathbf{t}^0 , ω^0 represent the nominal variables of traction and surface charge density, respectively and \mathbf{n}^0 is the unit vector normal to surface ∂B^0 .

Making reference back to the Eulerian formulation, when the surrounding space consists of vacuum (i.e. $B^{\text{sur}} \equiv B^*$), the stress in B^* reduces to Maxwell stress, here denoted by $\boldsymbol{\tau}^*$,

$$\boldsymbol{\tau}^* = \epsilon_0 \left(\mathbf{E}^* \otimes \mathbf{E}^* - \frac{1}{2}(\mathbf{E}^* \cdot \mathbf{E}^*)\mathbf{I} \right),$$

where symbol $*$ marks quantities evaluated in vacuum; moreover, electric displacement and electric field obey the law $\mathbf{D}^* = \epsilon_0 \mathbf{E}^*$, ϵ_0 being the permittivity of vacuum ($\epsilon_0 = 8.85$ pF/m). Field equations similar to (1) can be stated, which are more explicative if the two domains, B and B^* , are kept distinct:

$$\text{div } \boldsymbol{\tau} = \mathbf{0}, \quad \boldsymbol{\tau}^T = \boldsymbol{\tau}, \quad \text{div } \mathbf{D} = 0, \quad \text{curl } \mathbf{E} = \mathbf{0} \quad (\text{in } B), \quad (7)$$

$$\text{div } \mathbf{E}^* = 0, \quad \text{curl } \mathbf{E}^* = \mathbf{0} \quad (\text{in } B^*). \quad (8)$$

Here $\boldsymbol{\tau}$ explicitly refers to the total stress in B , while on the basis of equations (8) it can be easily shown that Maxwell stress is divergence-free (Dorfmann and Ogden, 2010), therefore, being the symmetry of $\boldsymbol{\tau}^*$ self-evident, equations (7) turn out to be formally

valid also in vacuum and can be extended to the whole space $B \cup B^*$. The associated boundary conditions are:

$$\boldsymbol{\tau} \mathbf{n} = \mathbf{t} + \boldsymbol{\tau}^* \mathbf{n} \quad (\text{on } \partial B_t), \quad \mathbf{v} = \tilde{\mathbf{v}} \quad (\text{on } \partial B_v), \quad (9)$$

$$\mathbf{D} \cdot \mathbf{n} = -\omega + \epsilon_0 \mathbf{E}^* \cdot \mathbf{n}, \quad \mathbf{n} \times (\mathbf{E} - \mathbf{E}^*) = \mathbf{0} \quad (\text{on } \partial B).$$

A Lagrangian version of the equations above can be provided for the dielectric body

$$\text{Div } \mathbf{S} = \mathbf{0}, \quad \mathbf{S} \mathbf{F}^T = \mathbf{F} \mathbf{S}^T, \quad \text{Div } \mathbf{D}^0 = 0, \quad \text{Curl } \mathbf{E}^0 = \mathbf{0} \quad (\text{in } B^0), \quad (10)$$

unlike for vacuum, as no deformation and therefore no Lagrangian variables can be defined there, thus conditions (8) still should be enforced in vacuum. Analogously, the boundary conditions are expressed with reference to Lagrangian and Eulerian variables inside the dielectric and vacuum, respectively

$$\mathbf{S} \mathbf{n}^0 = \mathbf{t}^0 + J \boldsymbol{\tau}^* \mathbf{F}_b^{-T} \mathbf{n}^0, \quad \mathbf{D}^0 \cdot \mathbf{n}^0 = -\omega^0 + \epsilon_0 J \mathbf{F}_b^{-1} \mathbf{E}^* \cdot \mathbf{n}^0, \quad (11)$$

$$\mathbf{n}^0 \times \mathbf{E}^0 = \mathbf{n}^0 \times \mathbf{F}_b^T \mathbf{E}^*, \quad (12)$$

where the notation $\mathbf{F}_b = \mathbf{F}|_{\partial B^0}$ has been introduced.

2.2 Constitutive equations

We consider a conservative material, whose response can be described through a free-energy function $W = W(\mathbf{F}, \mathbf{D}^0)$ as

$$\mathbf{S} = \frac{\partial W}{\partial \mathbf{F}}, \quad \mathbf{E}^0 = \frac{\partial W}{\partial \mathbf{D}^0}, \quad (13)$$

or, in the case contemplated hereafter of an incompressible material (the dielectric elastomer is assumed to be incompressible, being characterized by changes in shape typically much more significant than changes in volume), as

$$\mathbf{S} = \frac{\partial W}{\partial \mathbf{F}} - p \mathbf{F}^{-T}, \quad \mathbf{E}^0 = \frac{\partial W}{\partial \mathbf{D}^0}, \quad (14)$$

where p represents an unknown hydrostatic pressure; the total stress $\boldsymbol{\tau}$ and the current electric field \mathbf{E} can be easily obtained making use of eqs. (3) and (4).

Isotropy requires that $W(\mathbf{F}, \mathbf{D}^0)$ be a function of the invariants of the right Cauchy-Green tensor $\mathbf{C} = \mathbf{F}^T \mathbf{F}$, (note that here $I_3 = \det \mathbf{C} = 1$)

$$I_1 = \text{tr } \mathbf{C}, \quad I_2 = \frac{1}{2} [(\text{tr } \mathbf{C})^2 - \text{tr } \mathbf{C}^2], \quad (15)$$

and of three additional invariants depending on \mathbf{D}^0 , namely

$$I_4 = \mathbf{D}^0 \cdot \mathbf{D}^0, \quad I_5 = \mathbf{D}^0 \cdot \mathbf{C} \mathbf{D}^0, \quad I_6 = \mathbf{D}^0 \cdot \mathbf{C}^2 \mathbf{D}^0, \quad (16)$$

so that W is a function of five independent scalars. In particular, we will focus on the following form of the free energy

$$W(I_i) = W_{\text{elas}}(I_1, I_2) + \frac{1}{2\epsilon_0\bar{\epsilon}_r}(\bar{\gamma}_0 I_4 + \bar{\gamma}_1 I_5 + \bar{\gamma}_2 I_6), \quad (17)$$

where $\bar{\epsilon}_r$ is the relative dielectric constant of the material in the undeformed state ($\mathbf{F} = \mathbf{I}$) and $\bar{\gamma}_i$ ($i = 0, 1, 2$) are dimensionless constants, such that $\sum_i \bar{\gamma}_i = 1$. In general, these coefficients can be, in turn, function of the same invariants, however we do not take into account the more general form here, as (17) well captures the behaviour of ideal dielectrics and electrostrictive materials, adopting constant coefficients. Note that when electrostatic effects vanish (i.e. $I_4 = I_5 = I_6 = 0$), the free energy reduces to W_{elas} .

The combination of eqs. (14) and (17)¹ after the derivatives of the invariants² in terms of \mathbf{F} and \mathbf{D}^0 have been carried out and replaced, provides an explicit expression for the total stresses and electric fields. In particular the Lagrangian variables are

$$\begin{aligned} \mathbf{S} = & -p \mathbf{F}^{-T} + \mu [\bar{\alpha}_1 \mathbf{F} - \bar{\alpha}_2 (I_1 \mathbf{F} - \mathbf{F} \mathbf{C})] + \\ & + \frac{1}{\epsilon_0 \bar{\epsilon}_r} [\bar{\gamma}_1 \mathbf{F} \mathbf{D}^0 \otimes \mathbf{D}^0 + \bar{\gamma}_2 (\mathbf{F} \mathbf{D}^0 \otimes \mathbf{C} \mathbf{D}^0 + \mathbf{F} \mathbf{C} \mathbf{D}^0 \otimes \mathbf{D}^0)], \end{aligned} \quad (18)$$

$$\mathbf{E}^0 = (\mathcal{E}^0)^{-1} \mathbf{D}^0, \quad \text{where} \quad (\mathcal{E}^0)^{-1} = \frac{1}{\epsilon_0 \bar{\epsilon}_r} (\bar{\gamma}_0 \mathbf{I} + \bar{\gamma}_1 \mathbf{C} + \bar{\gamma}_2 \mathbf{C}^2), \quad (19)$$

being \mathcal{E}^0 the Lagrangian tensor of dielectric constants; the Eulerian variables are obtained through eqs. (3) and (4),

$$\begin{aligned} \boldsymbol{\tau} = & -p \mathbf{I} + \mu [\bar{\alpha}_1 \mathbf{B} - \bar{\alpha}_2 (I_1 \mathbf{B} - \mathbf{B}^2)] + \\ & + \frac{1}{\epsilon_0 \bar{\epsilon}_r} [\bar{\gamma}_1 \mathbf{D} \otimes \mathbf{D} + \bar{\gamma}_2 (\mathbf{D} \otimes \mathbf{B} \mathbf{D} + \mathbf{B} \mathbf{D} \otimes \mathbf{D})], \end{aligned} \quad (20)$$

$$\mathbf{E} = \boldsymbol{\mathcal{E}}^{-1} \mathbf{D}, \quad \text{where} \quad \boldsymbol{\mathcal{E}}^{-1} = \frac{1}{\epsilon_0 \bar{\epsilon}_r} (\bar{\gamma}_0 \mathbf{B}^{-1} + \bar{\gamma}_1 \mathbf{I} + \bar{\gamma}_2 \mathbf{B}), \quad (21)$$

with the definition of tensor $\boldsymbol{\mathcal{E}}$, such as $\boldsymbol{\mathcal{E}}^{-1} = \mathbf{F}^{-T} (\mathcal{E}^0)^{-1} \mathbf{F}^{-1}$, including the current dielectric constants. In the equations above, where, if necessary, we will label with a superscript ‘el’ (i.e. *electric*) the second row of eqs. (18) and (20), $\mu \bar{\alpha}_1 = 2\partial W / \partial I_1$ and $\mu \bar{\alpha}_2 = -2\partial W / \partial I_2$, being μ the shear modulus in the undeformed state and \mathbf{B} represents the left Cauchy-Green strain tensor; note that the hydrostatic pressure p is indeterminate

¹ Note that function $W_{\text{elas}}(I_1, I_2)$ has been assumed with no interconnection between invariants I_1 and I_2 , such that $\partial^2 W_{\text{elas}} / \partial I_1 \partial I_2 = 0$.

² Derivatives of the invariants:

$$\begin{aligned} \partial I_1 / \partial \mathbf{F} &= 2\mathbf{F}, \quad \partial I_2 / \partial \mathbf{F} = 2(I_1 \mathbf{F} - \mathbf{F} \mathbf{C}), \\ \partial I_4 / \partial \mathbf{F} &= \underline{0}, \quad \partial I_5 / \partial \mathbf{F} = 2(\mathbf{F} \mathbf{D}^0 \otimes \mathbf{D}^0), \quad \partial I_6 / \partial \mathbf{F} = 2[(\mathbf{F} \mathbf{D}^0 \otimes (\mathbf{C} \mathbf{D}^0) + (\mathbf{F} \mathbf{C} \mathbf{D}^0) \otimes \mathbf{D}^0], \\ \partial I_4 / \partial \mathbf{D}^0 &= 2\mathbf{D}^0, \quad \partial I_5 / \partial \mathbf{D}^0 = 2\mathbf{C} \mathbf{D}^0, \quad \partial I_6 / \partial \mathbf{D}^0 = 2\mathbf{C}^2 \mathbf{D}^0. \end{aligned}$$

and is evaluated enforcing the boundary conditions of the electro-elastic boundary-value problem. Variable \tilde{p} can be introduced as an alternative to p , such that $p = \tilde{p} + \mathbf{E} \cdot \mathbf{D}/2$, in accordance with what done by Zhao et al. (2007).

In general, as long as the hypotheses underlying expression (17) of the free energy are valid, (20)-(21) provide the general response of an isotropic nonlinear electroelastic soft solid encompassing a deformation-dependent electric – *electrostrictive* – response. Relation (21) shows that the behaviour of an ideal dielectric, for which the permittivity is independent of the current strain, i.e. $\mathbf{E} = \mathbf{D}/(\epsilon_0 \epsilon_r)$, is recovered imposing $\bar{\gamma}_0 = \bar{\gamma}_2 = 0$ and $\bar{\gamma}_1 = 1$, with $\bar{\epsilon}_r = \epsilon_r$. In this case, it is easy to notice that the association of the term multiplied by $\bar{\gamma}_1$ in (20) and of the contribution $\mathbf{E} \cdot \mathbf{D}/2$ included in the hydrostatic pressure p is recognizable as the internal Maxwell stress. In general, while coefficient $\bar{\gamma}_0$ accounts for a purely dielectric contribution, $\bar{\gamma}_2$ couples electrostriction to the mechanical response, as evident in the total stress law.

As the soft dielectrics typically in use are mainly silicones and acrylic elastomers, two appropriate constitutive models are Mooney-Rivlin and Gent (other models are likewise suitable, for instance Ogden and Arruda-Boyce models), respectively based on the following forms of elastic energy:

$$W_{\text{elas}}^{\text{MR}} = \frac{\mu_1}{2}(I_1 - 3) - \frac{\mu_2}{2}(I_2 - 3), \quad \mu = \mu_1 - \mu_2 \quad (\mu_2 < 0), \quad (22)$$

$$W_{\text{elas}}^{\text{G}} = -\frac{\mu}{2} J_m \ln \left[1 - \frac{I_1 - 3}{J_m} \right]. \quad (23)$$

Note that J_m is the value taken by invariant $I_1 - 3$ when the molecular chains of the internal network of the polymer are fully stretched; if the maximum stretch in a uniaxial test is taken to be 10, as suggested in Gent (1996), it turns out that $J_m = 97.2$, providing $\lambda_{\text{max}} = 9.959$ in a plane-strain uniaxial test. For the models above we have:

- Mooney-Rivlin model: $\bar{\alpha}_1 = \mu_1/\mu, \quad \bar{\alpha}_2 = \mu_2/\mu,$
- Gent model: $\bar{\alpha}_1 = \frac{J_m}{J_m - (I_1 - 3)}, \quad \bar{\alpha}_2 = 0.$

2.3 Deformation-dependent permittivity: electrostriction

Electrostriction is a term historically associated with the attitude of a material (polymeric or ceramic) to be deformed by the application of an electric field. In DEs, due to the large strains involved, this phenomenon concerns the variability of the dielectric permittivity with the deformation (Zhao and Suo, 2008). Typical materials employed for DE actuators are characterized by this property (Wissler and Mazza, 2007) and therefore it becomes important to investigate its effects towards the behaviour of such devices. In particular, our goal is, firstly, to show that electrostriction is included in the constitutive model described above leading to equations (18), (19) or (20), (21) and, secondly, to apply such equations in order to study the stability of DE actuators.

The considered sets of parameters $\bar{\gamma}_i$ ($i = 0, 1, 2$) have been assessed gathering data from the experimental tests performed by Wissler and Mazza (2007) and Li et al. (2011b)

Set # (Reference)	$\bar{\epsilon}_r$	$\bar{\gamma}_0$	$\bar{\gamma}_1$	$\bar{\gamma}_2$
1 (Wissler and Mazza, 2007)	4.68	0.00104	1.14904	-0.15008
2 (Li et al., 2011b)	4.5	0.00458	1.3298	-0.33438

Table 1: Sets of electrostrictive parameters employed in the instability analyses.

on 3M VHB4910 equally biaxially prestretched films. For this purpose, formula $(21)_2$ has been used to fit the experimental data, as depicted in Fig. 2a where the in-plane stretches are equal ($\lambda_1 = \lambda_2$), providing the values reported in Table 1.

The effect of electrostriction on the stress-strain behaviour of a soft dielectric layer is illustrated in Fig. 2b, where an equi-biaxial test ($\lambda_1 = \lambda_2$) for an actuator activated imposing an electric displacement field D_3 along the transverse direction is studied. There, the difference of the electric stress $\tau_{11}^{\text{el}} - \tau_{33}^{\text{el}}$ ($\tau_{11}^{\text{el}} = \tau_{22}^{\text{el}}$) is sketched in dimensionless form. For $\lambda_1 = \lambda_2 > 2$, the three curves remain almost parallel. It is clear that the difference in the electromechanical response is appreciable even in the neighbourhood of the natural configuration ($\lambda_1 = \lambda_2 = 1$).

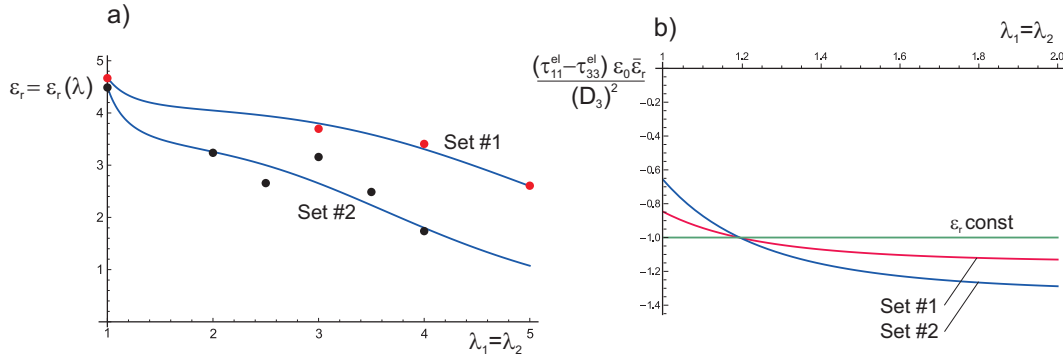


Figure 2: a) Fitting results based on expression $(21)_2$ of the experimental data on electrostriction of 3M VHB4910 provided by Wissler and Mazza (2007) and Li et al. (2011b) (see Table 1 for the values of the parameters $\bar{\gamma}_i$, $i = 0, 1, 2$). b) Effect of the electrostriction on the biaxial ‘electric’ stress-stretch response (‘el’ denotes the part of the stress depending on the electrostrictive parameters, see eq. (20)).

3 Incremental electro-elastic boundary-value problem

The investigation of instabilities developing in dielectrics at large strains is carried out superposing incremental deformations upon a given state of finite deformation (described in Section 2.1). Here we briefly introduce the topic, referring to Bertoldi and Gei (2011) for more details.

Again the general case is firstly presented, with the surrounding domain occupied by a different dielectric medium. Let us assume a perturbation $\dot{\mathbf{t}}^0$ and $\dot{\omega}^0$ of tractions and

surface charges applied on ∂B^0 (henceforth a superposed dot will denote the increment of the relevant quantity induced by the perturbation), leading the system to a new equilibrium configuration. According to the Lagrangian formulation, eqs. (5) and (6) hold true, as the body force density \mathbf{b}^0 is unchanged. The incremental problem is thus governed by the system

$$\text{Div } \dot{\mathbf{S}} = \underline{0}, \quad \text{Div } \dot{\mathbf{D}}^0 = 0, \quad \text{Curl } \dot{\mathbf{E}}^0 = \underline{0} \quad (\text{in } B^0 \cup B^{0\text{sur}}), \quad (24)$$

with incremental jump conditions at the external boundary of the body taking the form

$$[[\dot{\mathbf{x}}]] = \underline{0}, \quad [[\dot{\mathbf{S}}]] \mathbf{n}^0 = \dot{\mathbf{t}}^0 \quad (\text{on } \partial B_t^0), \quad \dot{\mathbf{x}} = \underline{0} \quad (\text{on } \partial B_v^0), \quad (25)$$

$$[[\dot{\mathbf{D}}^0]] \cdot \mathbf{n}^0 = -\dot{\omega}^0, \quad \mathbf{n}^0 \times [[\dot{\mathbf{E}}^0]] = \underline{0} \quad (\text{on } \partial B^0),$$

being $\dot{\mathbf{x}} = \dot{\chi}(\mathbf{x}^0)$ the incremental deformation associated with the incremental deformation gradient $\dot{\mathbf{F}} = \text{Grad} \dot{\chi}$.

Assuming that all incremental quantities are sufficiently small, the constitutive equations for a compressible medium (13) can be linearized as

$$\dot{S}_{iJ} = C_{iJkL}^0 \dot{F}_{kL} + B_{iJL}^0 \dot{D}_L^0, \quad \dot{E}_M^0 = B_{iJM}^0 \dot{F}_{iJ} + A_{ML}^0 \dot{D}_L^0, \quad (26)$$

where the components of the three electroelastic moduli tensors are given by

$$C_{iJkL}^0 = \frac{\partial^2 W}{\partial F_{iJ} \partial F_{kL}}, \quad B_{iJM}^0 = \frac{\partial^2 W}{\partial F_{iJ} \partial D_M^0}, \quad A_{ML}^0 = \frac{\partial^2 W}{\partial D_M^0 \partial D_L^0}. \quad (27)$$

From this definition, the following symmetries are derived:

$$C_{iJkL}^0 = C_{kLiJ}^0, \quad A_{ML}^0 = A_{LM}^0. \quad (28)$$

For incompressible materials ($\text{tr} \dot{\mathbf{F}} \mathbf{F}^{-1} = 0$, i.e. $\text{div} \dot{\mathbf{x}} = 0$), the incremental total first Piola-Kirchhoff stress tensor is given by

$$\dot{S}_{iJ} = C_{iJkL}^0 \dot{F}_{kL} + p F_{Li}^{-1} \dot{F}_{kL} F_{Jk}^{-1} - \dot{p} F_{Ji}^{-1} + B_{iJL}^0 \dot{D}_L^0. \quad (29)$$

The explicit expressions for the electroelastic moduli are detailed in Appendix A.

An updated Lagrangian formulation can be similarly provided for the incremental problem, based on the following field equations

$$\text{div } \boldsymbol{\Sigma} = \underline{0}, \quad \text{div } \hat{\mathbf{D}} = 0, \quad \text{curl } \hat{\mathbf{E}} = \underline{0} \quad (\text{in } B \cup B^{\text{sur}}), \quad (30)$$

where $\boldsymbol{\Sigma} = J^{-1} \dot{\mathbf{S}} \mathbf{F}^T$, $\hat{\mathbf{D}} = J^{-1} \mathbf{F} \dot{\mathbf{D}}^0$ and $\hat{\mathbf{E}} = \mathbf{F}^{-T} \dot{\mathbf{E}}^0$ correspond to incremental updated variables obtained through a push-forward operation from the corresponding Lagrangian incremental variables (see (3) and (4)). Identifying $\mathbf{u}(\mathbf{x}) = \dot{\mathbf{x}}$, the associated incremental boundary conditions read

$$[[\mathbf{u}]] = \underline{0}, \quad [[\boldsymbol{\Sigma}]] \mathbf{n} dA = \dot{\mathbf{t}}^0 dA^0 \quad (\text{on } \partial B_t), \quad \mathbf{u} = \underline{0} \quad (\text{on } \partial B_v), \quad (31)$$

$$[[\hat{\mathbf{D}}]] \cdot \mathbf{n} dA = -\dot{\omega}^0 dA^0, \quad \mathbf{n} \times [[\hat{\mathbf{E}}]] = \mathbf{0} \quad (\text{on } \partial B).$$

Note that also the incremental electric field is conservative, both in Lagrangian and Eulerian formulation, what guarantees the existence of relevant incremental electrostatic potentials.

Also in the frame of the updated Lagrangian formulation, the incremental constitutive equations turn out to be linear and, assuming $\mathbf{L} = \text{grad} \mathbf{u}$, take the form

$$\Sigma_{ir} = C_{irks} L_{ks} + B_{irk} \hat{D}_k, \quad \hat{E}_i = B_{kri} L_{kr} + A_{ik} \hat{D}_k. \quad (32)$$

The expression of the incremental constitutive tensors is straightforwardly derivable from eqs. (26) and (32) through the definition of the updated Lagrangian variables, giving

$$C_{irks} = \frac{1}{J} C_{iJkL}^0 F_{rJ} F_{sL}, \quad B_{irk} = B_{iJM}^0 F_{rJ} F_{Mk}^{-1}, \quad A_{ik} = J A_{JM}^0 F_{Ji}^{-1} F_{Mk}^{-1}, \quad (33)$$

where the following symmetry properties hold true:

$$C_{irks} = C_{ksir}, \quad B_{irk} = B_{rik}, \quad A_{ik} = A_{ki}. \quad (34)$$

Note that conditions (34)_{1,3} are analogous to (28)_{1,2}, while (34)₂ can be established by using the incremental form of the balance of angular momentum, also leading to condition

$$C_{iqkr} + \tau_{ir} \delta_{qk} = C_{qikr} + \tau_{qr} \delta_{ik}. \quad (35)$$

In the case of an incompressible material, while symmetries (34) still hold true, the updated version of the incremental first Piola-Kirchhoff total stress tensor becomes

$$\Sigma_{ir} = C_{irks} L_{ks} + p L_{ri} - \dot{p} \delta_{ir} + B_{irk} \hat{D}_k \quad (36)$$

while condition (35) turns into

$$C_{iqkr} + (\tau_{ir} + p \delta_{ir}) \delta_{qk} = C_{qikr} + (\tau_{qr} + p \delta_{qr}) \delta_{ik}. \quad (37)$$

The detailed expressions of the moduli for the updated Lagrangian formulation is reported in Appendix A.

In the case the domain outside the solid is vacuum ($B^{\text{sur}} \equiv B^*$), boundary conditions can be stated as in Dorfmann and Ogden (2010) and Bertoldi and Gei (2011). Here we consider the case, relevant for practical applications, where both surface tractions \mathbf{t}^0 and surface charges ω^0 are independent of the deformation (dead loading), thus $\dot{\mathbf{t}}^0 = \mathbf{0}$ and $\dot{\omega}^0 = 0$, while the electric field in vacuum vanish, as in the space outside a parallel-plate capacitor (by neglecting the edge effects). The consequence is that both the Maxwell stress $\boldsymbol{\tau}^*$ and its increment $\dot{\boldsymbol{\tau}}^*$, generally given as

$$\dot{\boldsymbol{\tau}}^* = \epsilon_0 \left[\dot{\mathbf{E}}^* \otimes \mathbf{E}^* + \mathbf{E}^* \otimes \dot{\mathbf{E}}^* - (\mathbf{E}^* \cdot \dot{\mathbf{E}}^*) \mathbf{I} \right],$$

vanish, while the increments of \mathbf{D}^* and \mathbf{E}^* (required in order to satisfy the incremental boundary conditions) are simply related as $\dot{\mathbf{D}}^* = \epsilon_0 \dot{\mathbf{E}}^*$. Therefore, also including the incompressibility of the dielectric, the boundary conditions for the Lagrangian formulation of the incremental problem specialize as follows

$$\dot{\mathbf{S}}\mathbf{n}^0 = \underline{0}, \quad \dot{\mathbf{D}}^0 \cdot \mathbf{n}^0 = \epsilon_0 (\mathbf{F}_b^{-1} \dot{\mathbf{E}}^*) \cdot \mathbf{n}^0, \quad \mathbf{n}^0 \times \dot{\mathbf{E}}^0 = \mathbf{n}^0 \times \mathbf{F}_b^T \dot{\mathbf{E}}^*, \quad (38)$$

while, with reference to updated Lagrangian variables, they read:

$$\boldsymbol{\Sigma}\mathbf{n} = \underline{0}, \quad \hat{\mathbf{D}} \cdot \mathbf{n} = \epsilon_0 \dot{\mathbf{E}}^* \cdot \mathbf{n}, \quad \mathbf{n} \times \hat{\mathbf{E}} = \mathbf{n} \times \dot{\mathbf{E}}^*. \quad (39)$$

Note that, owing to eq. (30)₃, the incremental electric variable $\dot{\mathbf{E}}^*$ in B^* is profitably defined making use of the incremental electrostatic potential in vacuum $\dot{\phi}^*(x_1, x_2)$ as $\dot{E}_i^* = -\dot{\phi}_{,i}^*$; the fulfilment of condition (30)₂ in B^* furthermore requires that the potential function is harmonic:

$$\dot{\phi}_{,ii}^* = 0. \quad (40)$$

4 Homogeneous fundamental paths: prestressed and prestretched layers

Two states of electromechanical finite, plane-strain deformations are considered for a dielectric elastomer layer of initial thickness h_0 , as anticipated in Sect. 1 and depicted in Fig. 1. With reference to the current configuration, let x_1 and x_2 be the longitudinal and the transverse axes associated with the orthonormal basis $\{\mathbf{e}_1, \mathbf{e}_2\}$ (being \mathbf{e}_3 the out-of-plane normal), respectively, such that the boundaries of the layer correspond to $x_2 = 0, h$, as shown in Fig. 3. We assume that the layer is infinitely wide and undergoes a homogeneous electric actuation aligned with direction \mathbf{e}_2 in the current configuration, i.e. $\mathbf{D} = D_2 \mathbf{e}_2$, with null external electric field, thus $\mathbf{E}^* = \mathbf{D}^* = \underline{0}$. The deformation state is still homogeneous with deformation gradient $\mathbf{F} = \text{diag}(\lambda, 1/\lambda, 1)$. The foreseen electrical activation can be achieved applying a uniform distribution of opposite surface charges on the two boundaries, in this case the absolute value of D_2 corresponds to the current charge density, see eq. (2)₄. The configuration can be also reached imposing a voltage between two perfectly compliant electrodes placed on the two surfaces, but the bifurcation analysis requires an incremental problem where the voltage is the varied electrical quantity.

4.1 Elongation under constant longitudinal force

In this case (path A in Fig. 1) the actuator is stress free along direction x_2 and subjected to a constant force $\tilde{S}h_0$ along the longitudinal direction, so that the nominal stress state is represented by

$$S_{11} = \tilde{S}, \quad S_{22} = 0, \quad (41)$$

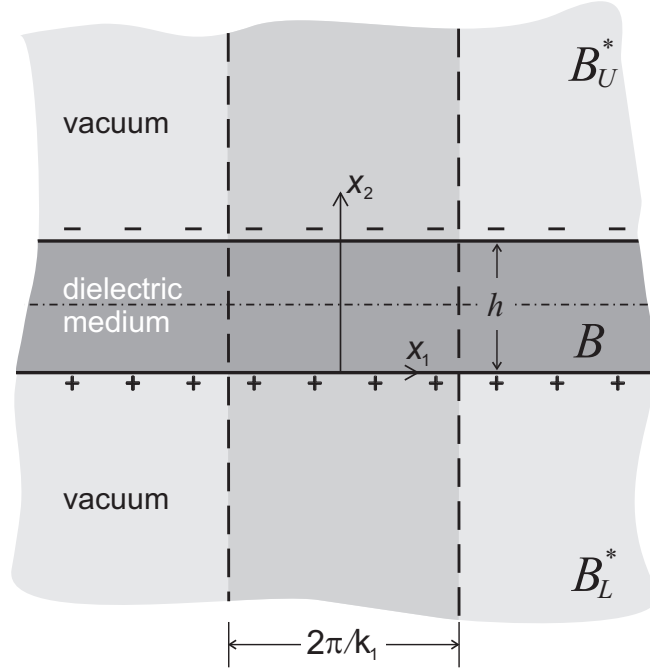


Figure 3: The general problem under study and the modular domain taken into account for the investigation of diffuse mode instability, according to the hypothesis of a periodic perturbation with wavelength equal to $2\pi/k_1$.

which provide the following implicit relation between λ and $\bar{D} = D_2/\sqrt{\mu\epsilon_0\bar{\epsilon}_r}$

$$\frac{\tilde{S}}{\mu}\lambda^2 + (\bar{\alpha}_1 - \bar{\alpha}_2) \left(\frac{1}{\lambda} - \lambda^3 \right) + \bar{D}^2 \left(\bar{\gamma}_1\lambda + \frac{2\bar{\gamma}_2}{\lambda} \right) = 0. \quad (42)$$

Graphical representations of this loading path are provided in Figs. 6a and 7a for electrostrictive Gent materials based on the two sets of parameters mentioned above, where the dimensionless electric displacement \bar{D} is reported on the vertical axis of both plots.

4.2 Pre-stretched specimen

The so-called path B depicted in Fig. 1 is characterized by a total stress component along direction x_2 identically vanishing throughout the solid, namely $\tau_{22} = 0$, with the layer longitudinally prestretched at $\lambda = \lambda_{\text{pre}}$ through the uniaxial tensile state of stress

$$\tau_{11}^{\text{pre}} = \mu(\bar{\alpha}_1 - \bar{\alpha}_2) \left(\lambda_{\text{pre}}^2 - \frac{1}{\lambda_{\text{pre}}^2} \right). \quad (43)$$

When an increasing electric displacement D_2 is subsequently superposed, the longitudinal stress changes as

$$\frac{\tau_{11}}{\mu} = \frac{\tau_{11}^{\text{pre}}}{\mu} - \bar{D}^2 \left(\bar{\gamma}_1 + \frac{2\bar{\gamma}_2}{\lambda_{\text{pre}}^2} \right). \quad (44)$$

The electric actuation yields a decrease in the longitudinal stress, therefore as shown in Figs. 6c and 7c (representing eq. (44) for Gent materials with the two considered sets of parameters), for increasing D_2 , τ_{11} becomes negative involving a buckling-like (diffuse-mode) instability. Condition $\tau_{11} = 0$ is referred to as ‘null tension’ threshold.

5 Global instabilities of a soft dielectric elastomer

Global equilibrium bifurcations for a generic electroelastic system consisting of two media, respectively occupying domains B^0 and $B^{0\text{sur}}$ with reference to a Lagrangian description can be addressed referring to the general theory introduced by Bertoldi and Gei (2011). Among this class of instabilities, for the electroelastic layer, we aim to investigate both electromechanical (pull-in) and diffuse-mode bifurcations, involving the relevant cases of buckling-like and surface-like instabilities.

Along an electromechanical loading path, the existence of two distinct solutions of the incremental problem is admitted and the fields generated as their difference, here denoted by symbol Δ (e.g. $\Delta\dot{\mathbf{x}} = \dot{\mathbf{x}}^{(1)} - \dot{\mathbf{x}}^{(2)}$), are taken into account. The difference fields can be regarded as the solution to a homogeneous incremental boundary-value problem (no associated incremental body forces, tractions, volume free charges, surface charges), thus an application of the principle of the virtual work in the material description requires that

$$\int_{B^0 \cup B^{0\text{sur}}} [\Delta\dot{\mathbf{S}} \cdot \Delta\dot{\mathbf{F}} + \Delta\dot{\mathbf{E}}^0 \cdot \Delta\dot{\mathbf{D}}^0] dV^0 = 0 \quad (45)$$

for every set of admissible Lagrangian fields $\{\Delta\dot{\mathbf{x}}, \Delta\dot{\mathbf{D}}^0, \Delta\dot{\mathbf{S}}, \Delta\dot{\mathbf{E}}^0\}$. Note that the existence of the integrals on $B^{0\text{sur}}$ requires the decay at infinity of the fields involved.

Being both $\dot{\mathbf{t}}^0$ and $\dot{\omega}^0$ null, the trivial pair $\{\dot{\mathbf{x}}^{(2)}, \dot{\mathbf{D}}^{0(2)}\} = \mathbf{0}$ represents a possible solution associated with the incremental boundary-value problem, consequently the difference fields reduce to the solution identified by superscript $^{(1)}$ and equation (45) can be given the following form:

$$\int_{B^0 \cup B^{0\text{sur}}} [\dot{\mathbf{S}}^{(1)} \cdot \dot{\mathbf{F}}^{(1)} + \dot{\mathbf{E}}^{0(1)} \cdot \dot{\mathbf{D}}^{0(1)}] dV^0 = 0. \quad (46)$$

Therefore, denoting by t ($t \geq 0$) the scalar loading parameter relevant to the principal equilibrium path, a sufficient condition preventing the dielectric layer from the occurrence of a bifurcation is

$$\int_{B^0 \cup B^{0\text{sur}}} [\dot{\mathbf{S}}(t) \cdot \dot{\mathbf{F}} + \dot{\mathbf{E}}^0(t) \cdot \dot{\mathbf{D}}^0] dV^0 > 0, \quad (47)$$

while a bifurcation takes place at $t = t_{cr}$ as soon as, for an admissible critical pair $\{\dot{\mathbf{x}}_{cr}, \dot{\mathbf{D}}_{cr}^0\}$ –the *primary eigenmode*–, the functional becomes positive semi-definite so that equation (46) becomes true, namely

$$\int_{B^0 \cup B^{0\text{sur}}} [\dot{\mathbf{S}}_{cr}(t_{cr}) \cdot \dot{\mathbf{F}}_{cr} + \dot{\mathbf{E}}_{cr}^0(t_{cr}) \cdot \dot{\mathbf{D}}_{cr}^0] dV^0 = 0, \quad (48)$$

with $\dot{\mathbf{S}}_{cr}(t_{cr})$ and $\dot{\mathbf{E}}_{cr}^0(t_{cr})$ given by the incremental constitutive equations.

The instability criterion defined in eq. (48) according to the Lagrangian description can be easily given an updated Lagrangian expression through a formal push-forward operation, namely

$$\int_{B \cup B^{\text{sur}}} [\boldsymbol{\Sigma}_{cr}(t_{cr}) \cdot \mathbf{L}_{cr} + \hat{\mathbf{E}}_{cr}(t_{cr}) \cdot \hat{\mathbf{D}}_{cr}] dV = 0, \quad (49)$$

for an admissible critical pair $\{\mathbf{u}_{cr}, \hat{\mathbf{D}}_{cr}\}$. Admissibility of \mathbf{u}_{cr} and $\hat{\mathbf{D}}_{cr}$ requires the fulfilment of field and boundary conditions, namely the incompressibility constraint, $\text{div } \mathbf{u}_{cr} = 0$, as well as eqs. (31)_{1,3,4} and (30)₂. Therefore, starting with an admissible critical pair $\{\mathbf{u}_{cr}, \hat{\mathbf{D}}_{cr}\}$ and using eqs. (32) with the introduction of $\mathbf{L}_{cr} = \text{grad } \mathbf{u}_{cr}$ to compute the corresponding incremental equilibrated total stress and curl-free electric field $\boldsymbol{\Sigma}_{cr}$ and $\hat{\mathbf{E}}_{cr}$ (respectively satisfying field eqs. (30)₁ and (30)₃), imposing the critical condition (49) is equivalent to the enforcement of the boundary conditions (31)_{2,5} in weak form, as can be easily shown making use of divergence and Stokes' theorems.

When the surrounding medium is vacuum, condition (49) takes the form

$$\int_B [\boldsymbol{\Sigma}_{cr} \cdot \mathbf{L}_{cr} + \hat{\mathbf{E}}_{cr} \cdot \hat{\mathbf{D}}_{cr}] dV + \int_{B^*} \dot{\mathbf{E}}_{cr}^* \cdot \dot{\mathbf{D}}_{cr}^* dV = 0, \quad (50)$$

which can be simplified as

$$\int_B [\boldsymbol{\Sigma}_{cr} \cdot \mathbf{L}_{cr} + \hat{\mathbf{E}}_{cr} \cdot \hat{\mathbf{D}}_{cr}] dV + \epsilon_0 \int_{\partial B^*} \dot{\phi}_{cr}^* \text{grad } \dot{\phi}_{cr}^* \cdot \mathbf{n} dA = 0, \quad (51)$$

through equation (40), entailing $\dot{\mathbf{E}}^* \cdot \dot{\mathbf{D}}^* = \epsilon_0 \text{div}(\dot{\phi}^* \text{grad } \dot{\phi}^*)$, and subsequent application of the divergence theorem to the integral on B^* in (50). Condition (51) can be further simplified with the integral on ∂B^* transported along ∂B , as will be shown later for the problem under study.

5.1 Electromechanical instability

This bifurcation may arise when the body is deformed homogeneously as effect of dead-load tractions/charges applied to its boundary, therefore homogeneous perturbation fields \mathbf{L} , $\hat{\mathbf{D}}$, and $\dot{\phi}^*$ are considered. Note that in this case the surface integral in (51) vanishes, being $\text{grad } \dot{\phi}^* = 0$, therefore, as a result of homogeneity, the instability criterion requires that the argument of the volume integral in (51) vanishes, namely, for an incompressible material,

$$\mathbb{C}(t) \mathbf{L} \cdot \mathbf{L} + p(t) \text{tr} \mathbf{L}^2 + 2\mathbf{B}(t) \hat{\mathbf{D}} \cdot \mathbf{L} + \mathbf{A}(t) \hat{\mathbf{D}} \cdot \hat{\mathbf{D}} = 0 \quad (52)$$

for at least a pair $\{\mathbf{L}, \hat{\mathbf{D}}\} = \{\mathbf{L}_{cr}, \hat{\mathbf{D}}_{cr}\} \neq \mathbf{0}$, with $\text{tr} \mathbf{L} = 0$.

Note that, for the sake of conciseness, subscript 'cr' has been omitted here and will be hereafter. Therefore, bifurcation is predicted in correspondence to the loss of positive definiteness of the quadratic form in eq. (52) (see Gei et al., 2012, for the application of this criterion to a homogeneous actuators and the comparison with the method based on the Hessian of the total energy).

5.2 Diffuse-mode instability

Diffuse modes, corresponding to a plane-strain inhomogeneous response of the layer with wavelength given by $2\pi/k_1$ (being k_1 the wave-number of the perturbation), are investigated. The extreme cases of *long-wavelength* ($k_1 \rightarrow 0$) and *surface instability* ($k_1 \rightarrow +\infty$), where the critical modes are strongly localized in the vicinity of the surface, are considered. Making reference to Fig. 3, diffuse bifurcation modes are described representing the set of admissible incremental fields in condition (51) as sinusoidal functions.

Considering the updated Lagrangian formulation, the incremental boundary-value problem can be written in scalar notation in the form:

$$\Sigma_{11,1} + \Sigma_{12,2} = 0, \quad \Sigma_{21,1} + \Sigma_{22,2} = 0, \quad \hat{D}_{1,1} + \hat{D}_{2,2} = 0, \quad \hat{E}_{1,2} - \hat{E}_{2,1} = 0 \quad (\text{in } B), \quad (53)$$

$$\dot{E}_i^* = -\dot{\phi}_{,i}^*, \quad \dot{\phi}_{,ii}^* = 0 \quad (i = 1, 2, \text{ in } B^*), \quad (54)$$

$$\Sigma_{12} = 0, \quad \Sigma_{22} = 0, \quad \hat{D}_2 = \epsilon_0 \dot{E}_2^*, \quad \hat{E}_1 = \dot{E}_1^* \quad (\text{along } \partial B). \quad (55)$$

The periodic solution adopted inside layer B ,

$$\begin{aligned} u_1(x_1, x_2) &= V s e^{sk_1 x_2} \cos k_1 x_1, & u_2(x_1, x_2) &= V e^{sk_1 x_2} \sin k_1 x_1, \\ \hat{D}_1(x_1, x_2) &= \delta s e^{sk_1 x_2} \cos k_1 x_1, & \hat{D}_2(x_1, x_2) &= \delta e^{sk_1 x_2} \sin k_1 x_1, \\ \dot{p}(x_1, x_2) &= Q e^{sk_1 x_2} \sin k_1 x_1, \end{aligned} \quad (56)$$

guarantees that both fields \mathbf{u} and $\hat{\mathbf{D}}$ are divergence-free, as required by incompressibility and eq. (53)₃ (note that in the case of a compressible dielectric, condition $\text{div} \mathbf{u} = 0$ would not subsist, but simultaneously variable \dot{p} would disappear).

In order to fulfil the remote decay conditions in the surrounding space, the relevant solution is expressed on the basis of the following harmonic electric potentials inside each of the portions B_U^* and B_L^* in which B^* has been split according to Fig. 3:

- $\dot{\phi}^*(x_1, x_2) = F_U \sin k_1 x_1 e^{-k_1 x_2} \quad \text{in } B_U^* = \{\mathbf{x} \in B^*, x_2 \geq h\},$
- $\dot{\phi}^*(x_1, x_2) = F_L \sin k_1 x_1 e^{+k_1 x_2} \quad \text{in } B_L^* = \{\mathbf{x} \in B^*, x_2 \leq 0\}.$

The interface jump condition (55)₃ at $x_2 = 0, h$ is easily satisfied through a convenient choice of constants F_U and F_L .

When modes (56) are plugged into constitutive eqs. (32)₂ and (36) and the resulting expressions into conditions (53)_{1,2,4}, a homogeneous system of equations for amplitudes V, δ, Q is generated:

$$\begin{bmatrix} k_1 s(-C_{1111} + C_{1122} + s^2 C_{1212} + C_{1221}) & s^2 B_{121} & -1 \\ -k_1(C_{2121} + s^2(C_{2112} + C_{2211} - C_{2222})) & s(-B_{211} + B_{222}) & -s \\ k_1 s(s^2 B_{121} + B_{211} - B_{222}) & s^2 A_{11} - A_{22} & 0 \end{bmatrix} \begin{bmatrix} V \\ \delta \\ Q \end{bmatrix} = \begin{bmatrix} 0 \\ 0 \\ 0 \end{bmatrix}.$$

Thus a non trivial solution is only admissible when the associated matrix of coefficients is singular, i.e. when the following cubic equation in s^2 is satisfied:

$$\Omega_6 s^6 + \Omega_4 s^4 + \Omega_2 s^2 + \Omega_0 = 0. \quad (57)$$

For the fundamental paths investigated throughout the paper, the expressions of the constitutive tensors A_{ik} , B_{irk} and C_{irks} reported in Appendix A and their symmetry properties (34), the coefficients of (57) can be given the following simplified expressions:

$$\begin{aligned}\Omega_6 &= -B_{121}^2 + A_{11}C_{1212}, \\ \Omega_4 &= -2B_{121}(B_{121} - B_{222}) - A_{22}C_{1212} - A_{11}(C_{1111} - 2C_{1122} - 2C_{1221} + C_{2222}), \\ \Omega_2 &= -(B_{121} - B_{222})^2 + A_{11}C_{2121} + A_{22}(C_{1111} - 2C_{1122} - 2C_{1221} + C_{2222}), \\ \Omega_0 &= -A_{22}C_{2121}.\end{aligned}\tag{58}$$

According to the nature of the six solutions s_i , different regimes can be identified and the general solution inside B is built by superposition:

$$\begin{aligned}u_1(x_1, x_2) &= \sum_{i=1}^6 V_i s_i e^{s_i k_1 x_2} \cos k_1 x_1, & u_2(x_1, x_2) &= \sum_{i=1}^6 V_i e^{s_i k_1 x_2} \sin k_1 x_1, \\ \hat{D}_1(x_1, x_2) &= \sum_{i=1}^6 \delta_i s_i e^{s_i k_1 x_2} \cos k_1 x_1, & \hat{D}_2(x_1, x_2) &= \sum_{i=1}^6 \delta_i e^{s_i k_1 x_2} \sin k_1 x_1, \\ \dot{p}(x_1, x_2) &= \sum_{i=1}^6 Q_i e^{s_i k_1 x_2} \sin k_1 x_1.\end{aligned}\tag{59}$$

The critical conditions are now determined introducing the latter expressions into the stability criterion, eq. (51), which can be further simplified by taking into account the bounded modular domain highlighted in Fig. 3 as

$$\begin{aligned}\int_{-\frac{\pi}{k_1}}^{\frac{\pi}{k_1}} \int_0^h [\boldsymbol{\Sigma} \cdot \mathbf{L} + \hat{\mathbf{E}} \cdot \hat{\mathbf{D}}] dx_2 dx_1 + \\ -\epsilon_0 \int_{-\frac{\pi}{k_1}}^{\frac{\pi}{k_1}} \left[\dot{\phi}^* \text{grad} \dot{\phi}^* \cdot \mathbf{n} \Big|_{x_2=h} + \dot{\phi}^* \text{grad} \dot{\phi}^* \cdot \mathbf{n} \Big|_{x_2=0} \right] dx_1 = 0;\end{aligned}\tag{60}$$

here \mathbf{n} denotes the outward normal unit vector relevant to the specific boundary portion of B (as in Sect. 2.1). Eq. (60) stems from the remote decay conditions of the electric fields inside vacuum and the periodic nature of the perturbation, allowing the integrals on ∂B^* to vanish along the vertical surfaces bounding the integration domain (corresponding to the dashed lines in Fig. 3). This procedure has been applied to the problem under study (the results will be presented in Sect. 7): the primary eigenmodes so obtained have been shown to coincide with those evaluated on the basis of the procedure illustrated in Bertoldi and Gei (2011), where all the boundary conditions (31) are enforced in strong form.

6 A local instability of soft dielectric elastomers: band-localization

A potential local instability mode arising in large-strain solid mechanics is band localization, where fields at bifurcation exhibit a discontinuity across a narrow band of unknown

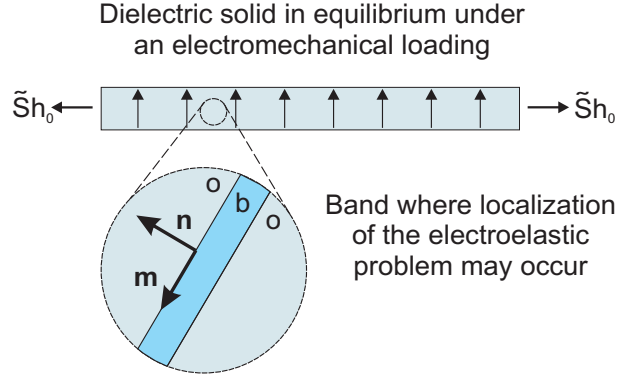


Figure 4: Band discontinuity in a homogeneously deformed dielectric elastomer. Band thickness is unpredictable on the basis of the proposed approach.

inclination. The condition for its onset along the homogeneous path (here reference will be made to the paths illustrated in Sect. 4) can be determined investigating the admissible jumps of the incremental quantities across the interface between the band (superscript ‘b’) and the rest of the solid (superscript ‘o’). In the current configuration, let \mathbf{n} and \mathbf{m} denote two orthogonal unit vectors ($\mathbf{n} \cdot \mathbf{m} = 0$), normal to the band interface the first and aligned with it the latter, as depicted in Fig. 4³.

Imagine that at the attainment of a threshold along the electro-mechanical loading path, \mathbf{L}^o and $\hat{\mathbf{D}}^o$ represent the uniform response of the solid to an incremental change in the boundary conditions except inside the band, where the incremental displacement \mathbf{u}^b is constant along the planes $\mathbf{x} \cdot \mathbf{n} = \text{const}$ and the incremental electric displacement $\hat{\mathbf{D}}^b$ is uniform. Compatibility relationships across the interface, namely $(\mathbf{L}^b - \mathbf{L}^o)\mathbf{m} = \mathbf{0}$ and continuity of the normal component of $\hat{\mathbf{D}}$, respectively, require that

$$\mathbf{L}^b = \mathbf{L}^o + \xi \mathbf{m} \otimes \mathbf{n}, \quad \hat{\mathbf{D}}^b = \hat{\mathbf{D}}^o + \zeta \mathbf{m}, \quad (61)$$

where ξ and ζ are real scalars representing mode amplitudes within the band; note the relative displacement field in $(61)_1$, associated with the dyadic $\mathbf{m} \otimes \mathbf{n}$, that corresponds to an isochoric simple shear of amount ξ . Both fields \mathbf{L}^b and $\hat{\mathbf{D}}^b$ are required to satisfy field equations (53) inside the band.

On the other hand, continuity of the increments of both traction and the tangential component of the electric field require

$$(\Sigma^b - \Sigma^o)\mathbf{n} = \mathbf{0}, \quad \hat{\mathbf{E}}^b - \hat{\mathbf{E}}^o = \beta \mathbf{n}, \quad (62)$$

where, again, β is a real variable. The use of (61) in the constitutive equations and in (62) provides, in component form, respectively

$$Q_{ik}m_k - \frac{1}{\xi}(\dot{p}^b - \dot{p}^o)n_i + \bar{\zeta}B_{iqa}m_a n_q = 0, \quad (63)$$

³The vector \mathbf{n} used here must not be confused with the outward normal to ∂B defined in Section 2.

$$B_{iqa}m_in_q + \bar{\zeta}A_{ab}m_b = \bar{\beta}n_a,$$

where $Q_{ik} = C_{ikp}n_p n_q$, $\bar{\zeta} = \zeta/\xi$ and $\bar{\beta} = \beta/\xi$. Further manipulation of (63) yields

$$\bar{\zeta} = -\frac{B_{iqa}m_in_q m_a}{A_{ab}m_a m_b}, \quad \bar{\beta} = B_{iqa}m_in_q n_a + \bar{\zeta}A_{ab}n_a m_b, \quad (64)$$

$$\frac{1}{\xi}(\dot{p}^b - \dot{p}^o) = Q_{ik}m_k n_i + \bar{\zeta}B_{iqa}n_in_q m_a,$$

as well as the condition for band localization, namely (assuming $A_{ab}m_a m_b \neq 0$)

$$A_{ab}Q_{ik}m_a m_b m_i m_k - (B_{iqa}m_in_q m_a)^2 = 0. \quad (65)$$

Eq. (65) clearly depends on the current state of finite-strain and on the normal to the band \mathbf{n} (the components of \mathbf{m} can be easily substituted according to relation $m_r = e_{sr}n_s$, where $e_{12} = -e_{21} = 1$, $e_{11} = e_{22} = 0$).

For the fundamental paths under study, eq. (65) explicitly becomes

$$\Gamma_6\nu^6 + \Gamma_4\nu^4 + \Gamma_2\nu^2 + \Gamma_0 = 0, \quad (66)$$

with the assumption $\nu = n_2/n_1$ ($n_1 \neq 0$) and the coefficients related to those in eq. (57) as:

$$\Gamma_6 = -\Omega_6, \quad \Gamma_4 = \Omega_4, \quad \Gamma_2 = -\Omega_2, \quad \Gamma_0 = \Omega_0.$$

Band localization occurs when eq. (66), which can be reduced to a cubic in the unknown ν^2 , admits a real solution ν^* . The real roots can be determined explicitly following Tartaglia-Cardano's theory (valid for $\Gamma_6 \neq 0$; when $\Gamma_6 = 0$, eq. (66) becomes a biquadratic and the roots can be easily obtained). According to the values taken by the discriminant

$$\Delta = \frac{a^2}{4} + \frac{b^3}{27}, \quad (67)$$

where

$$a = -\frac{1}{3}\left(\frac{\Gamma_4}{\Gamma_6}\right)^2 + \frac{\Gamma_2}{\Gamma_6}, \quad b = \frac{2}{27}\left(\frac{\Gamma_4}{\Gamma_6}\right)^3 - \frac{1}{3}\frac{\Gamma_2\Gamma_4}{\Gamma_6^2} + \frac{\Gamma_0}{\Gamma_6}, \quad (68)$$

two cases arise:

- when $\Delta \geq 0$, eq. (66) has only one real root, i.e.

$$\nu^2 = \sqrt[3]{-\frac{b}{2} + \sqrt{\Delta}} + \sqrt[3]{-\frac{b}{2} - \sqrt{\Delta}} - \frac{\Gamma_4}{3\Gamma_6}; \quad (69)$$

- when $\Delta < 0$, eq. (66) admits three real roots, namely

$$\nu_1^2 = 2\sqrt{-\frac{a}{3}}\cos\theta - \frac{\Gamma_4}{3\Gamma_6}, \quad (70)$$

$$\nu_2^2 = 2\sqrt{-\frac{a}{3}}\cos\left(\frac{\theta + 2\pi}{3}\right) - \frac{\Gamma_4}{3\Gamma_6}, \quad \nu_3^2 = 2\sqrt{-\frac{a}{3}}\cos\left(\frac{\theta + 4\pi}{3}\right) - \frac{\Gamma_4}{3\Gamma_6},$$

where $\theta = \arctan(-2\sqrt{-\Delta}/b)$ if $b \leq 0$ or $\theta = \pi + \arctan(-2\sqrt{-\Delta}/b)$ if $b > 0$.

Along the principal path, the onset of band localization corresponds to the fulfilment of one of the following conditions: i) $\Gamma_6 = 0$, ii) $\Gamma_0 = 0$, and iii) $\Delta = 0$. The adoption of free-energy (17) provides the following relation between λ and \bar{D} for case i)

$$\bar{D} = \sqrt{-\frac{(\bar{\alpha}_1 - \bar{\alpha}_2)(\bar{\gamma}_0 + \bar{\gamma}_1\lambda^2 + \bar{\gamma}_2\lambda^4)}{\bar{\gamma}_2^2 + \bar{\gamma}_0(\bar{\gamma}_1\lambda^2 + \bar{\gamma}_2(2 + \lambda^4))}}, \quad (71)$$

while for case ii) it gives

$$\bar{D} = \sqrt{-\frac{(\bar{\alpha}_1 - \bar{\alpha}_2)}{\bar{\gamma}_2}}. \quad (72)$$

Case iii) is more involved, but a condition analogous to the previous ones can be easily determined from (67).

In any case, at the onset, the amplitude ratios $\bar{\zeta}$ and $\bar{\beta}$ defined in eq. (64), become

$$\bar{\zeta} = -\frac{B_{121}\nu^3 + (B_{222} - B_{121})\nu}{A_{11}\nu^2 + A_{22}}n_1, \quad (73)$$

$$\bar{\beta} = B_{121} + (B_{222} - B_{121})\nu^2 + \bar{\zeta}(A_{22} - A_{11})\nu. \quad (74)$$

7 Results

7.1 Diffuse-mode instability

Diffuse-mode instability results are depicted in Fig. 5 for a prestretched specimen with different λ_{pre} (path B in Fig. 1), on the basis of an extended Gent electroelastic free energy (23), characterized by different sets of electrostrictive parameters (see Table 1). Both symmetric and antisymmetric modes (with respect to the symmetry axis of the layer, see Fig. 3; see also Bigoni and Gei, 2001) have been carefully checked and the critical conditions have always been proved to correspond to antisymmetric modes.

In all the plots the dimensionless electric displacement \bar{D} , acting as ‘electrical’ loading parameter, is plotted as a function of the dimensionless wavenumber k_1h ; note that the limit $k_1h \rightarrow \infty$ denotes a surface-like mode⁴, while low values of k_1h correspond to buckling-like modes. The latter case is well depicted by the graphical sketch of modes $k_1h = 0.4, 1.3$ in Fig. 1.

The effects of electrostriction onto the critical electric displacement at bifurcation are represented in part d) of Fig. 5, where the comparison between the computations displayed in parts a), b), c) is reported. In general, a high degree of electrostriction entails more evident reductions in the critical electric actuation (specially for $\lambda_{\text{pre}} = 1.5, 2.5$ that are levels of prestretch important in the applications). This can be justified observing that instability occurs when the axial stress τ_{11} , tensile just after the prestretching, becomes

⁴At high frequencies, the critical \bar{D} for symmetric and antisymmetric modes converges to the same value.

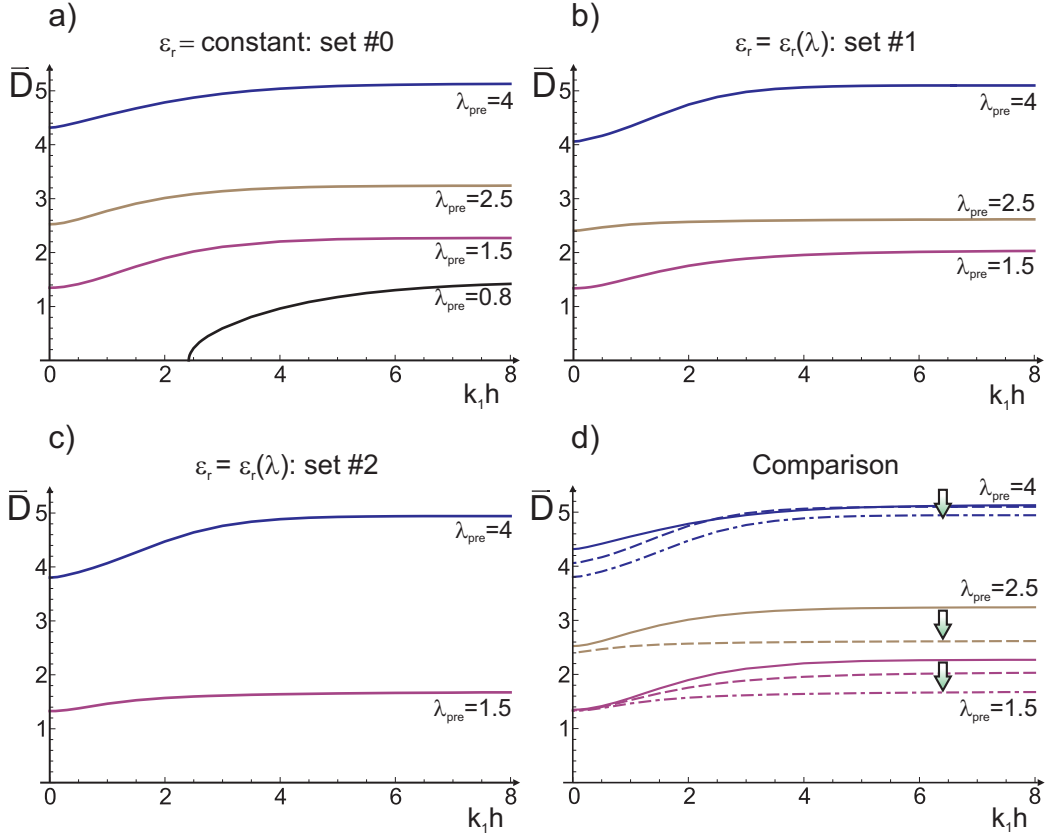


Figure 5: Diffuse instability modes for a prestretched actuator in plane strain (for a Gent material model). Parts a), b), c): critical dimensionless electric displacement \bar{D} vs dimensionless wavenumber $k_1 h$ for constant ϵ_r and for the two sets of electrostrictive parameters considered in Table 1 at different values of the applied prestretch λ_{pre} . The comparison reported in d) shows that electrostriction significantly lowers the critical \bar{D} . In c) the case $\lambda_{pre} = 2.5$ is not reported as it lies within a band-localization range (see Fig. 7).

compressive. As can be observed comparing two paths at the same λ_{pre} in parts c) of Figs. 6 and 7, at high electrostriction this event takes place for a slightly lower \bar{D} .

It is worth highlighting that experimental results on electrostriction are only available for stretched membranes (see Sect. 2.3), therefore the estimated values of parameters $\bar{\gamma}_i$ well interpolate the behaviour for $\lambda_{pre} > 1$, while for $\lambda_{pre} < 1$ we have noticed that the consequent dielectric constant ϵ_r is far from reasonable values. As a consequence, for $\lambda_{pre} = 0.8$ only the curve for constant ϵ_r has been sketched in Fig. 5 a). For Set #2, calculations show that at a prestretch $\lambda_{pre} = 2.5$ the specimen is in the conditions where, along the electromechanical deformation, band-localization instability first takes place and the previous homogenous response of the layer is lost (see below): for this reason the curve for $\lambda_{pre} = 2.5$ has not been illustrated.

7.2 Band-localization instability

Band-localization instability analysis for homogeneously deformed actuators is reported in Figs. 6, 7 for an extended Gent free-energy function with set of parameters #1 and #2, respectively, for both fundamental paths introduced in Sect. 4. In a) the actuator is prestressed with a given nominal traction \tilde{S} , following a nonlinear electroelastic deformation corresponding to path A, while in b) and c) the specimen is prestretched at $\lambda = \lambda_{\text{pre}}$ and then actuated (path B), as for the analysis of diffuse modes. In a), and c) dashed portions of the loading path curves (bounded by circles) denote ranges where band localization occurs. Even though the current analysis allows to predict only the onset of such instability, while nothing can be said about the evolution of the band, we note that in electroelasticity stable homogeneous nonlinear deformations are also possible beyond the theoretical emergence of the band, suggesting that the range of instability can be crossed in some way, in order to reach the stable path anew (the same applies to electroelastic deformations where the actuator deforms biaxially –computations not reported). Comparison with experiments is difficult, as we are not aware of papers dealing with electroelastic band-localization instability and this article provides the first theoretical analysis on the topic. The following comments must be added to clarify the key points of our investigation:

i) the onset of localization is strongly dependent on electrostriction. For a material with *deformation independent permittivity* (i.e. $\epsilon_r = \bar{\epsilon}_r$), no localization is predicted on the basis of eq. (66). Therefore, to detect the emergence of a band, accurate experiments must be carried out in order to carefully measure and identify the electrostrictive properties of the specimen. It is worth pointing out that Gent elastic model does not exhibit localization under pure mechanical loadings, thus the instabilities observed here are genuine electromechanical effects;

ii) polynomial (66) is obtained assuming $\hat{\mathbf{D}}$ as the independent electric incremental variable, what physically corresponds to perturb the surface charge applied on the layer boundaries⁵. Alternatively, a similar analysis can be carried out perturbing the voltage at the electrodes, therefore choosing $\hat{\mathbf{E}}$ as the primary variable. Even though the governing equations are the same, the analogous of (66) may exhibit properties being substantially different from those of (66), as the relevant constitutive equations accounting for the coupling differ from those presented in Sect. 3. This analysis is out of the scope of the present paper and will be developed elsewhere;

iii) a failure mode experimentally observed in DE actuators is electric breakdown: when the electric field inside the solid reaches a material-dependent threshold, the dielectric becomes conductive, with a discharge crossing the solid and inducing a strong localized damage to the actuator. We suggest that electric breakdown can be induced by a band-localization instability. Indeed, at the onset of this instability and for both fundamental paths, the band inclination predicted on the basis of our analysis has always proven to be orthogonal to the direction of the electric field (i.e. $\nu \rightarrow \infty$, while

⁵The technique assuming the control of the charge on the layer boundaries is less common than the one based on the control of the voltage applied by the electrodes, nevertheless it is possible and has been successfully employed by Keplinger et al. (2010).

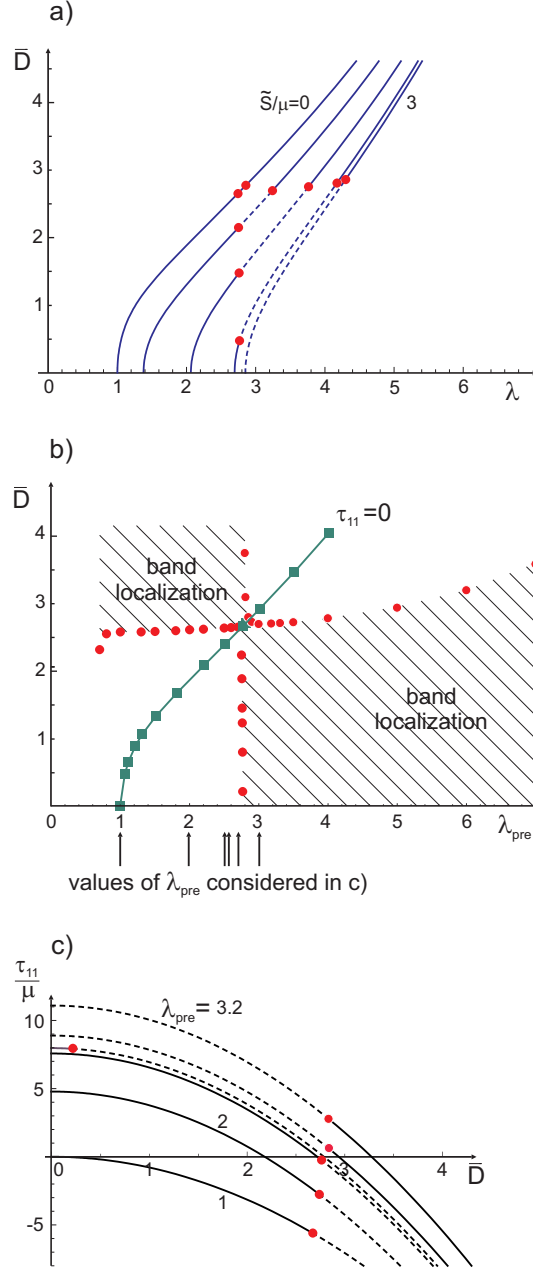


Figure 6: Band-localization instability analysis for an electrically actuated DE layer in plane strain (Gent material model, set of parameter #1, see Table 1). a): plot for prestressed actuators with different \tilde{S}/μ (path A, in ascending order $\tilde{S}/\mu = 0, 1, 2, 2.8, 3$); dashed lines indicate ranges where instability occurs (bounded by circles). b), c): results for actuators initially prestretched at $\lambda = \lambda_{\text{pre}}$ (path B). In particular, b): instability region in the $\lambda_{\text{pre}}-\bar{D}$ diagram – the line marked by squares corresponds to $\tau_{11} = 0$ (‘null tension’ threshold: beyond this line the specimen is compressed); c): dimensionless longitudinal stress (τ_{11}/μ) and localization ranges in terms of electrical actuation \bar{D} .

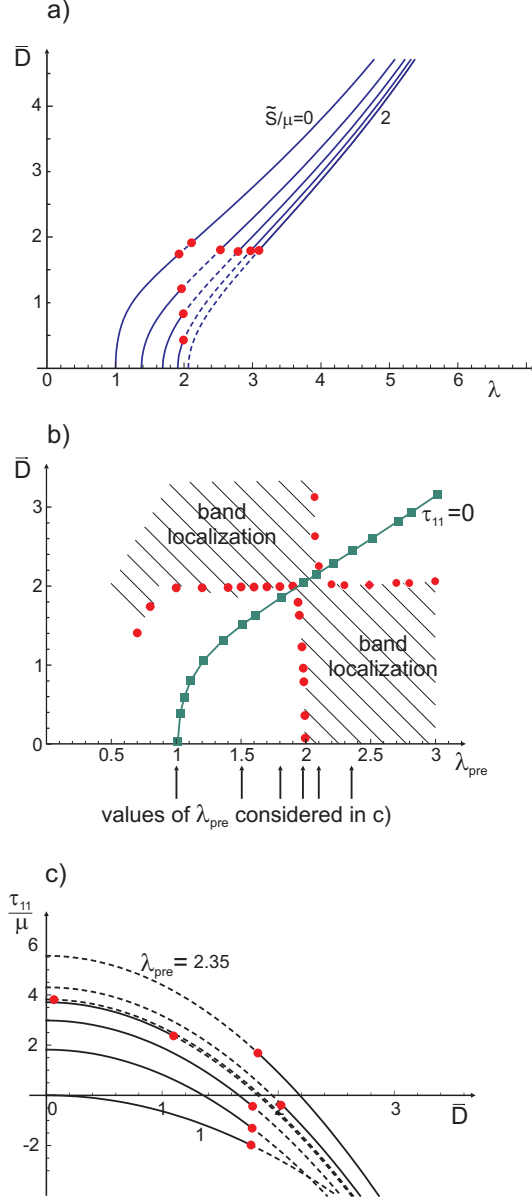


Figure 7: Band-localization instability analysis for an electrically actuated DE layer in plane strain (Gent material, set of parameter #2, see Table 1). a): plot for prestressed actuators with different \tilde{S}/μ (path A, in ascending order $\tilde{S}/\mu = 0, 1, 1.5, 1.8, 2$); dashed lines indicate ranges where instability occurs (bounded by circles). b), c): results for actuators initially prestretched at $\lambda = \lambda_{\text{pre}}$ (path B). In particular, b): instability region in the $\lambda_{\text{pre}}-\bar{D}$ diagram – the line marked by squares corresponds to $\tau_{11} = 0$ (‘null tension’ threshold: beyond this line the specimen is compressed); c): dimensionless longitudinal stress (τ_{11}/μ) and localization ranges in terms of electrical actuation \bar{D} .

coordinate x_2 , where the band develops, remains unknown). Through relationships (64) we can estimate the incremental fields inside the band by setting the amplitude ξ ; this has been done for the case $\tilde{S}/\mu = 0$ in Fig. 6a, showing that the increment of the electric field $\hat{\mathbf{E}}^b$ inside the band is almost six times larger than that outside (i.e., $\hat{\mathbf{E}}^o$), with a strong localized behaviour of the incremental electric field. This can obviously match with micromechanical issues in order to promote electric breakdown. From the previous considerations, it appears evident that the development of a band in a real sample represents something uncertain, requiring additional investigations, both experimental and theoretical. As for the latter aspect, it could be relevant to adopt a microelectromechanical model, in order to follow the evolution of the band and check the stability of the predicted shear bands.

Coming back to Fig. 6 (relevant to the set of parameters #1), for both fundamental paths it appears clear that $\lambda \approx 2.76$ provides a theoretical critical threshold. As anticipated, this limit strongly depends on the degree of electrostriction, as shown in Fig. 7 for set #2, where the same limit drops to approximately 1.97. For prestretched actuators similar considerations apply, as depicted in parts b) and c) of Figs. 6 and 7. In parts b), in addition to the regions where localization represents the theoretically critical condition, the line corresponding to a null longitudinal stress ($\tau_{11} = 0$, ‘null tension’ threshold, as an effect of electric actuation \bar{D}), is also reported, as typical devices must operate under a tensile stress state in order to avoid buckling instability. Therefore, only the points at the right-hand side of the line $\tau_{11} = 0$ correspond to sensible configurations for real actuators. The arrows below the horizontal axis in parts b) of both figures (ranging from $\lambda_{\text{pre}} = 1$ to $\lambda_{\text{pre}} = 3.2$ in Fig. 6 and between 1 and 2.35 in Fig. 7) refer to the loading paths indicated in part c).

7.3 Buckling instability: mechanically compressed vs prestretched and electrically activated slabs

Even though the bodies investigated in this paper are electrically activated, the diffuse-mode instabilities analysed in Sect. 5.2 are essentially driven by the induced compressive longitudinal stress arising as a reaction to the imposed boundary constraints. Therefore, it seems interesting to address the following question: which longitudinal stresses are responsible for a common buckling mode in two identical silicone-like specimens, mechanically loaded the former and electrically activated the latter? In order to provide an answer, an isotropic thin layer with constitutive behaviour described by a Mooney-Rivlin elastic energy is taken into account, for which two different plane strain fundamental paths are considered (same geometry as in Fig. 3): *i*) a purely mechanical longitudinal compression, i.e. $\lambda_{\text{pre}} < 1$ (but remaining in the neighbourhood of 1) with $\bar{D} = 0$; *ii*) an electric actuation ($\bar{D} > 0$) as in the path B described previously, with $\lambda_{\text{pre}} = 1$. The bifurcation analysis of the first problem is well-known (see Biot, 1965) and is summarized here as the continuous curve illustrated in Fig. 8, representing the compressive longitudinal true stress at the onset of instability (actually, when no electric effects are present, the total stress τ_{11} reduces to the Cauchy stress). The second problem has been studied

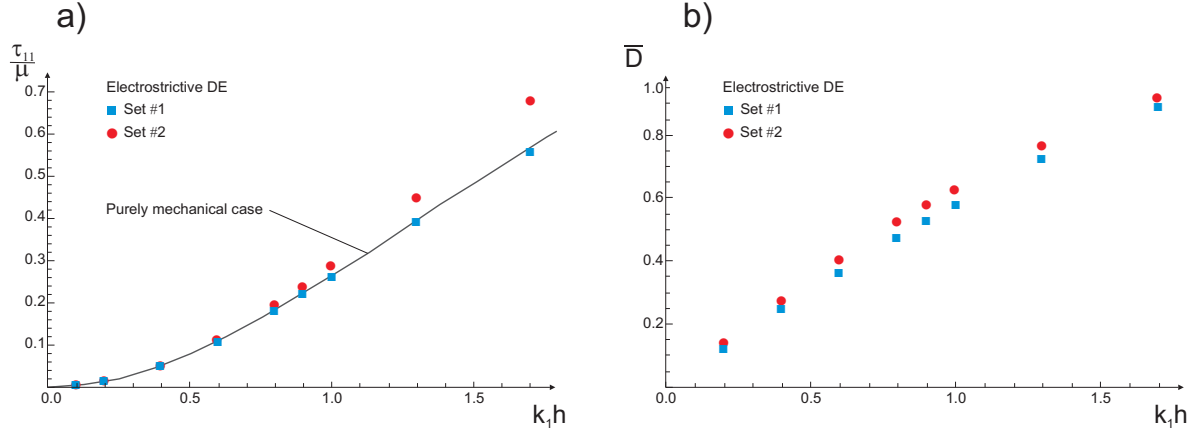


Figure 8: Buckling instability analysis in plane strain for a purely mechanically compressed (Mooney-Rivlin material) and an electrically actuated DE layer ($\lambda_{\text{pre}} = 1$, Mooney-Rivlin material, sets of parameters #1, 2, see Table 1). a): dimensionless longitudinal true stress for the mechanically compressed (continuous line: as $\bar{D} = 0$, τ_{11} reduces to the Cauchy stress) and the electromechanically activated DE (scattered points corresponding to the sets of parameters indicated in the legend) vs. the dimensionless wavenumber $k_1 h$. b): dimensionless electric displacement \bar{D} at instability vs. $k_1 h$ for the electromechanically activated DE.

like in Sect. 5.2, as the limit of two distinct problems with values of λ_{pre} approaching 1 from below and above, respectively, being a periodic solution as the one in (59) not admissible when $\lambda_{\text{pre}} = 1$. The so-calculated buckling conditions for the two sets of electrostrictive materials are superposed in Fig. 8: part a) shows the dimensionless total stresses, while in part b) the dimensionless electric displacement is pictured only for the electromechanical case. Note that for $k_1 h \ll 1$, for which the Eulerian instability theory is recovered, there is an outstanding agreement between the buckling stresses for the cases of both mechanically and electromechanically activated slab, while for higher $k_1 h$ appreciable differences arise. Interestingly, the higher distance between the continuous curve and the scattered points of Fig. 8a pertains to the material with the higher degree of electrostriction: this indicates that electrostriction strongly influences the instability of the DE specimen, while a non-electrostrictive DE structure essentially buckles at a compressive stress very similar to that required in the purely mechanical case.

8 Conclusions

In soft dielectric elastomers, the electric permittivity may change considerably with the strain as a result of a strain-dependent polarization response under an imposed electric field. This phenomenon is called *electrostriction* and this paper addresses its modelling in the framework of the general nonlinear theory of isotropic electroelasticity for both large and incremental deformations. After having identified the relevant material parameters with experimental data, in the second part of the article the general theory of bifurcation

for electroelastic body proposed by Bertoldi and Gei (2011) is applied to investigate mainly diffuse-mode bifurcations and band-localization instability, for which a detailed analysis is described for the first time, showing that the theoretical condition for its existence is only met when the dielectric solid displays an electrostrictive behaviour, being excluded otherwise.

Results show that electrostriction may activate the former modes at a threshold up to 30% lower than that for an ideal dielectric (for which the permittivity is constant), while we can argue that band-localization may trigger electric breakdown and failure of actual prestretched/prestressed specimens. However, further theoretical and experimental investigations are needed to clarify how localization may develop within a DE actuator under various electromechanical loading conditions.

In the final part, a comparison between the buckling stresses of a mechanical compressed slab and the electrically activated counterpart is performed, revealing that a high degree of electrostriction increases the critical stress and stiffens the layer compared to the purely mechanical problem.

Acknowledgements. The financial supports of PRIN grant no. 2009XWLFKW, financed by Italian Ministry of Education, University and Research, and of the COST Action MP1003 ‘European Scientific Network for Artificial Muscles’, financed by EU, are gratefully acknowledged.

References

- [1] A. Ask, A. Menzel and M. Ristinmaa. Phenomenological modeling of viscous electrostrictive polymers. *International Journal of Non-Linear Mechanics* 47, 156-165, 2012.
- [2] A. Ask, R. Denzer, A. Menzel and M. Ristinmaa. Inverse-motion-based form finding for quasi-incompressible finite electroelasticity. *International Journal for Numerical Methods in Engineering* 94, 554–572, 2013.
- [3] Y. Bar-Cohen (Ed). *Electroactive Polymer (EAP) Actuators as Artificial Muscles*. SPIE Press, Bellingham, Wa., 2001.
- [4] K. Bertoldi and M. Gei, Instability in multilayered soft dielectrics. *J. Mech. Phys. Solids* 59, 18–42, 2011.
- [5] D. Bigoni and M. Gei. Bifurcation of a coated, elastic cylinder. *Int. J. Solids Structures* 38, 5117-5148, 2001.
- [6] D. Bigoni and F. Dal Corso. The unrestrainable growth of a shear band in a pre-stressed material. *Proc. R. Soc. Lond. A* 464, 2365-2390, 2008.

- [7] M.A. Biot. Mechanics of incremental deformations. J. Wiley & Sons, New York, 1965.
- [8] P. Brochu and Q. Pei. Advances in Dielectric Elastomers for Actuators and Artificial Muscles. *Macromolecular Rapid Communications* 31, 10-36, 2010.
- [9] F. Carpi, D. De Rossi, R. Kornbluh, R. Pelrine and P. Sommer-Larsen (Eds). *Dielectric Elastomers as Electromechanical Transducers*. Elsevier, Oxford, UK, 2008a.
- [10] F. Carpi, G. Gallone, F. Galantini and D. De Rossi. Silicone-poly(hexylthiophene) blends as elastomers with enhanced electromechanical transduction properties. *Adv. Funct. Mat.* 18, 235-241, 2008b.
- [11] G. deBotton, L. Tevet-Deree and E.A. Socolsky. Electroactive heterogeneous polymers: analysis and applications to laminated composites. *Mech. Adv. Mat. Struct.* 14, 13-22, 2007.
- [12] D. De Tommasi, G. Puglisi, G. Saccomandi and G. Zurlo. Pull-in and wrinkling instabilities of electroactive dielectric actuators. *J. Physics D: Appl. Phys.* 43, 325501, 2010.
- [13] D. De Tommasi, G. Puglisi and G. Zurlo. Electromechanical instability and oscillating deformations in electroactive polymer films. *Appl. Phys. Lett.* 102, 011903, 2013.
- [14] A. Dorfmann and R.W. Ogden. Nonlinear electroelasticity. *Acta Mech.* 174, 167-183, 2005.
- [15] A. Dorfmann and R.W. Ogden. Nonlinear electroelastostatics: incremental equations and stability. *Int. J. Eng. Sci.* 48, 1-14, 2010.
- [16] M. Gei, S. Roccabianca and M. Bacca. Controlling band gap in electroactive polymer-based structures. *IEEE-ASME Trans. Mechatron.* 16, 102107, 2011.
- [17] M. Gei, S. Colonnelli and R. Springhetti. A framework to investigate instabilities of homogeneous and composite dielectric elastomer actuators. *Electroactive Polymer Actuators and Devices, SPIE Conference 8340*, Ed. Bar-Cohen, San Diego, Ca, U.S.A., paper 834010, 2012.
- [18] M. Gei, R. Springhetti and E. Bortot. Performance of soft dielectric laminated composites. *Smart Materials and Structures* 22, 104014, 2013.
- [19] A.N. Gent. A new constitutive relation for rubber. *Rubber Chem. Techol.* 69, 59-61, 1996.
- [20] R. Hill and J.W. Hutchinson. Bifurcation phenomena in the plane tension test. *J. Mech. Phys. Solids* 23, 239-264, 1975.

- [21] C. Huang, Q.M. Zhang, G. deBotton and K. Bhattacharya. All-organic dielectric-percolative three-component composite materials with high electromechanical response. *Appl. Phys. Lett.* 84, 4391-4393, 2004.
- [22] C. Keplinger, M. Kaltenbrunner, N. Arnold and S. Bauer. Rontgen’s electrode-free elastomer actuators without electromechanical pull-in instability. *PNAS* 107, 4505–4510, 2010.
- [23] B. Li, L. Liu and Z. Suo. Extension limit, polarization saturation, and snap-through instability of dielectric elastomers. *International Journal of Smart and Nano Materials* 2, 59-67, 2011a.
- [24] B. Li, H. Chen, J. Qiang, S. Hu, Z. Zhu and Y. Wang. Effect of mechanical pre-stretch on the stabilization of dielectric elastomer actuation. *J. Phys. D: Appl. Phys.* 44, 155301, 2011b.
- [25] R.M. McMeeking and C.M. Landis. Electrostatic forces and stored energy for deformable dielectric materials. *J. Appl. Mech.* 72, 581–590, 2005.
- [26] M. Molberg, D. Crespy, P. Rupper, F. Nuesch, J.-A.E. Manson, C. Lowe and D.M. Opris. High Breakdown field dielectric elastomer actuators using encapsulated polyaniline as high dielectric constant filler. *Adv. Funct. Mater.* 20, 3280-3291, 2010.
- [27] A. Nobili and L. Lanzoni. Electromechanical instability in layered materials. *Mech. Materials* 42, 582–592, 2010.
- [28] R. Pelrine, R. Kornbluh and J. Joseph. Electrostriction of polymer dielectrics with compliant electrodes as a means of actuation. *Sens. Act. A* 64, 77-85, 1998.
- [29] R. Pelrine, R. Kornbluh, Q. Pei and J. Joseph. High-speed electrically actuated elastomers with strain greater than 100%. *Science* 287, 836-839, 2000.
- [30] P. Ponte Castaneda and M.H. Siboni. A finite-strain constitutive theory for electroactive polymer composites via homogenization. *Int. J. Nonlinear Mech.* 47, 293-306, 2012.
- [31] J.R. Rice. The initiation and growth of shear bands. In *Plasticity and soil mechanics* (ed. A.C. Palmer), Cambridge University Engineering Department, Cambridge, UK, 1973, pp. 263-274.
- [32] S. Risse, B. Kussmaul, H. Kruger and G. Kofod. Synergistic improvement of actuation properties with compatibilized high permittivity filler. *Adv. Funct. Mater.* 22, 3958-3962, 2012.
- [33] S. Rudykh and G. deBotton. Stability of anisotropic electroactive polymers with application to layered media. *ZAMP* 62, 1131–1142, 2011.

- [34] G. Shmuel, M. Gei and G. deBotton. The Rayleigh-Lamb wave propagation in a dielectric layer subjected to large deformations. *International Journal of Non-linear Mechanics* 47, 307–316, 2012.
- [35] Z. Suo, X. Zhao and W.H. Greene. A nonlinear field theory of deformable dielectrics. *J. Mech. Phys. Solids* 56, 467-486, 2008.
- [36] L. Tian, L. Tevet–Deree, G. deBotton and K. Bhattacharya. Dielectric elastomer composites. *J. Mech. Phys. Solids* 60, 181–198, 2012.
- [37] R. Vertechy, A. Frisoli, M. Bergamasco, F. Carpi, G. Frediani and D. De Rossi. Modeling and experimental validation of buckling dielectric elastomer actuators. *Smart Mater. Struct.* 21, 094005, 2012.
- [38] M. Wissler and E. Mazza. Electromechanical coupling in dielectric elastomer actuators. *Sens. Actuators A* 138, 384–393, 2007.
- [39] Q.M. Zhang, H. Li, M. Poh, F. Xia, Z.-Y. Cheng, H. Xu and C. Huang. An all-organic composite actuator material with a high dielectric constant. *Nature* 419, 284-289, 2002.
- [40] X. Zhao, W. Hong and Z. Suo. Electromechanical hysteresis and coexistent states in dielectric elastomers. *Phys. Rev. B* 76, 134113, 2007.
- [41] X. Zhao and Z. Suo. Electrostriction in elastic dielectrics undergoing large deformation. *J. Appl. Phys.* 104, 123530, 2008.

Appendix A - Incremental constitutive moduli for the class of free energies represented by (17).

Total Lagrangian formulation.

$$A_{MN}^0 = \frac{1}{\epsilon_0 \bar{\epsilon}_r} \left(\bar{\gamma}_0 \delta_{MN} + \bar{\gamma}_1 C_{MN} + \bar{\gamma}_2 C_{MN}^2 \right), \quad (75)$$

$$B_{iJM}^0 = \frac{1}{\epsilon_0 \bar{\epsilon}_r} \left[\bar{\gamma}_1 (F_{iM} D_J^0 + F_{iS} D_S^0 \delta_{JM}) + \right. \\ \left. + \bar{\gamma}_2 (F_{iM} C_{JS} D_S^0 + F_{iS} C_{JM} D_S^0 + F_{iS} C_{SM} D_J^0 + F_{iR} C_{RS} D_S^0 \delta_{JM}) \right], \quad (76)$$

$$\begin{aligned}
C_{iJkL}^0 = & \mu \left[\bar{\alpha}_1 \delta_{ik} \delta_{JL} + 2F_{iJ} F_{kL} \left(\frac{\partial \bar{\alpha}_1}{\partial I_1} - \bar{\alpha}_2 \right) + \right. \\
& -2 \frac{\partial \bar{\alpha}_2}{\partial I_2} (I_1 F_{iJ} - F_{iR} C_{RJ}) (I_1 F_{kL} - F_{kS} C_{SL}) + \\
& -\bar{\alpha}_2 [\delta_{ik} (I_1 \delta_{JL} - C_{JL}) - F_{iL} F_{kJ} - B_{ik} \delta_{JL}] + \\
& \left. + 2 \frac{\partial \bar{\alpha}_1}{\partial I_2} (2I_1 F_{iJ} F_{kL} - F_{iM} C_{MJ} F_{kL} - F_{iJ} F_{kM} C_{ML}) \right] + \\
& + \frac{1}{\epsilon_0 \bar{\epsilon}_r} \left[\bar{\gamma}_1 \delta_{ik} D_J^0 D_L^0 + \bar{\gamma}_2 [\delta_{ik} D_S^0 (C_{JS} D_L^0 + C_{LS} D_J^0) + \right. \\
& \left. + F_{iR} D_R^0 (\delta_{JL} F_{kS} D_S^0 + F_{kJ} D_L^0) + F_{iL} F_{kS} D_S^0 D_J^0 + B_{ik} D_J^0 D_L^0 \right].
\end{aligned} \tag{77}$$

Updated Lagrangian formulation.

$$A_{ab} = \frac{1}{\epsilon_0 \bar{\epsilon}_r} \left(\bar{\gamma}_0 B_{ab}^{-1} + \bar{\gamma}_1 \delta_{ab} + \bar{\gamma}_2 B_{ab} \right), \tag{78}$$

$$B_{iqa} = \frac{1}{\epsilon_0 \bar{\epsilon}_r} \left[\bar{\gamma}_1 (\delta_{ia} D_q + D_i \delta_{qa}) + \bar{\gamma}_2 (\delta_{ia} B_{qs} D_s + B_{qa} D_i + B_{ia} D_q + B_{is} D_s \delta_{qa}) \right], \tag{79}$$

$$\begin{aligned}
C_{iqkp} = & \mu \left[\bar{\alpha}_1 \delta_{ik} B_{pq} + 2B_{iq} B_{kp} \left(\frac{\partial \bar{\alpha}_1}{\partial I_1} - \bar{\alpha}_2 \right) + \right. \\
& -2 \frac{\partial \bar{\alpha}_2}{\partial I_2} (I_1 B_{iq} - B_{is} B_{sq}) (I_1 B_{kp} - B_{pt} B_{tk}) + \\
& -\bar{\alpha}_2 (\delta_{ik} (I_1 B_{pq} - B_{pt} B_{tq}) - B_{ip} B_{kq} - B_{ik} B_{pq}) + \\
& \left. 2 \frac{\partial \bar{\alpha}_1}{\partial I_2} (2I_1 B_{iq} B_{kp} - B_{is} B_{sq} B_{kp} - B_{iq} B_{ks} B_{sp}) \right] + \\
& + \frac{1}{\epsilon_0 \bar{\epsilon}_r} \left[\bar{\gamma}_1 \delta_{ik} D_p D_q + \bar{\gamma}_2 \left(\delta_{ik} D_s (B_{qs} D_p + B_{ps} D_q) + D_i (B_{pq} D_k + B_{qk} D_p) + \right. \right. \\
& \left. \left. + D_q (B_{pi} D_k + B_{ik} D_p) \right) \right].
\end{aligned} \tag{80}$$